General Disclaimer

One or more of the Following Statements may affect this Document

- This document has been reproduced from the best copy furnished by the organizational source. It is being released in the interest of making available as much information as possible.

- This document may contain data, which exceeds the sheet parameters. It was furnished in this condition by the organizational source and is the best copy available.

- This document may contain tone-on-tone or color graphs, charts and/or pictures, which have been reproduced in black and white.

- This document is paginated as submitted by the original source.

- Portions of this document are not fully legible due to the historical nature of some of the material. However, it is the best reproduction available from the original submission.

APPLICATION OF MULTIVARIABLE SEARCH TECHNIQUES

TO THE OPTIMIZATION OF AIRFOILS IN A

LOW SPEED NONLINEAR INVISCID FLOW FIELD

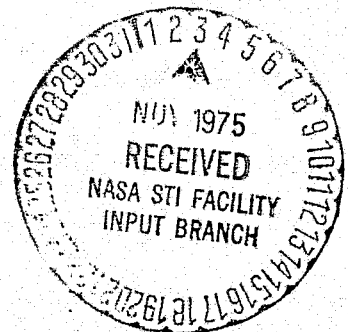### JULY 1975

CONTRACT NAS 2-8599

DONALD S. HAGUE

ANTONY W. MERZ

Prepared by

AEROPHYSICS RESEARCH CORPORATION

Bellevue, Washington   98009

Originally Published as

Aerophysics Research Corporation TN-206

TABLE OF CONTENTS

TABLE OF CONTENTS (cont'd)

LIST OF FIGURES

LIST OF FIGURES (cont'd)

LIST OF TABLES

APPLICATION OF MULTIVARIABLE SEARCH TECHNIQUES

TO THE OPTIMIZATION OF AIRFOILS IN A

LOW SPEED NONLINEAR INVISCID FLOW FIELD

By D. S. Hague and A. W. Merz

SUMMARY

Multivariable search techniques are applied to a
particular class of airfoil optimization problems. These
are the maximization of lift and the minimization of dis-
turbance pressure magnitude in an inviscid nonlinear flow
field. A variety of multivariable search techniques contained
in an existing non-linear optimization code, AESOP, are
applied to this design problem. These techniques include
elementary single parameter perturbation methods, organized
search such as steepest-descent, quadratic, and Davidon
methods, randomized procedures, and a generalized search
acceleration technique. Airfoil design variables are
seven in number and define perturbations to the profile of
an existing NACA airfoil. The relative efficiency of the
techniques are compared. It is shown that elementary one
parameter at a time and random techniques compare favorably
with organized searches in the class of problems considered.
It is also shown that significant reductions in disturbance
pressure magnitude can be made while retaining reasonable
lift coefficient values at low free stream Mach numbers.

The optimal solutions reported here were obtained by application of a generalized multivariable search code, AESOP, orginally constructed under contract to the National Aeronautics and Space Administration's Office of Advanced Research and Development.   Original documentation of this code is given in references 1 to 3; an outline of the analysis underlying this code is presented below.

MULTIVARIABLE SEARCH

The general non-linear multivariable optimization problem is concerned with the maximization or minimization of a *pay-off* or *performance function* of the form

$$\phi = \phi(\alpha_i), \quad i = 1, 2, \ldots, N \tag{1}$$

Subject to an array of constraints

$$C_j = C_j(\alpha_i) = 0, \quad j = 1, 2, \ldots, p \tag{2}$$

The α_i are the *independent variables* whose values are to be determined so as to maximize or minimize the performance function $\phi(\alpha_i)$ subject to the constraints of equation (2). The α_i may be looked upon as the components of a *control vector*, $\bar{\alpha}$, in a space R^N of dimension N. Since maximization of a function is equivalent to minimization with a change of sign, it suffices to discuss the case in which the performance function is to be *minimized*.

Multivariable optimization problems involving *inequality constraints* may also be encountered. If the constraints are applied directly to the independent variables

$$\alpha_i^L < \alpha_i < \alpha_i^H \tag{3}$$

the inequality constraints define a region of the control space within which the solution must lie. Inequality constraints on *functions of the independent variables* similarly restrict the region in which the optimal solution is to be obtained. In this case

$$E_k^L(\alpha_i) < E_k(\alpha_i) < E_k^H(\alpha_i) \tag{4}$$

Inequality constraints can be used to restrict the search region directly, or, alternatively, they may be applied in an indirect fashion by a *transformation to equality constraints*. Several transformations may be used for this purpose. For example, let an equality constraint, C_k, be defined by the transformation

$$C_k = \begin{cases} (E_k^L - E_k)^2, & E_k < E_k^L \\ 0, & E_k^L < E_k < E_k^H \\ (E_k^H - E_k)^2, & E_k^H < E_k \end{cases} \tag{5}$$

3

Constraining C_k to zero will result in the constraint of equation (4) being satisfied.

Problems involving equality constraints can be treated as unconstrained problems by replacing the actual performance function, $\phi(\alpha_i)$, by an *augmented performance function*, ϕ^*, where

$$\phi^* = \phi + \sum_{j=1}^{P} U_j C_j^2 \tag{6}$$

It can be shown that, provided the positive weighting constants U_j are sufficiently large in magnitude, minimization of the performance function subject to the constraints, equation (2), is equivalent to minimization of the unconstrained penalized performance function defined by equation (6). This approach permits search techniques for finding unconstrained minima to be applied in the solution of constrained minima problems *at the cost of some increased complexity* in the behavior of the performance function, the performance *response surface*. In practical application, the weighting constants U_j are determined *adaptively* on the basis of response surface behavior.

Alternatives to this approach are available, notably Bryson's approach to the steepest-descent search, reference 4. This method has been exploited in connection with the numerical solution of variational problems encountered in the optimization of aerospace vehicle flight paths, references 5, 6, and 7. However, the use of such techniques implies *smoothness* of the response surface. This smoothness may not be present in general; hence, the AESOP code is limited to the less restrictive penalty function approach of equation (6)

4

Numerical Solution of Non-Linear Multivariable
Optimization Problems

This section is devoted to a discussion of the search
algorithms for solution of non-linear multivariable optimi-
zation problems available in the AESOP code. A wide variety
of search algorithms have been devised for the solution of
multivariable optimization problems. Many of these algorithms
are restricted to the solution of linear or quadratic problems.
Algorithms of this type must be supplemented by more general
search procedures if generality of solution is sought; for
engineering problems tend to lead to non-linear formulation
with the possibility of discontinuities in both the performance
function response surface and its derivative. Most of the
searches which prove effective in these problems combine a
direction generating algorithm,such as steepest-descent, with
with a one-dimensional search. Distance traversed through
the control space in the selected direction is measured by a
step-size, or perturbation parameter, DP. The object of the
one-dimensional search is to determine the value of DP which
minimizes the performance function along the chosen ray and to
establish the corresponding control vector.

In practice, the diverse nature of non-linear multivariable
optimization problems leads to the conclusion that no one
search algorithm can be uniquely described as being the "best"
in all the situations which may be encountered. Rather, a
combination of searches, some of which may be of quite elemen-
tary nature, provides the most reliable and economical conver-
gence to the optimal solution.

<u>One-dimensional search</u>. Multivariable search problems
are reduced to one-dimensional problems whenever a search
algorithm is used to establish a one-to-one correspondence
between the control vector and a single scalar perturbation
parameter, (DP). In such a situation

$$\alpha_i = \alpha_i(DP), \quad i = 1, 2, \ldots, N \qquad (7)$$

so that equation (1) becomes

$$\phi = \phi(\alpha_i) = \phi(DP) \qquad (8)$$

Similarly, the right hand sides of equations (2) and (6)
become functions of the scalar perturbation parameter.

The relationship, equation (7), specifies a ray through
the control space. As noted above, the objective of the
one-dimensional search along this ray is to locate the value
of DP which provides the minimum performance function value.

Numerical search for the one-dimensional minima can be
carried out in a local fashion, by the Newton-Raphson method,
for example, or by a global search of the ray throughout the
feasible region. The localized polynomial approximation is
appropriate to the *terminal convergence phase* in a problem
solution when some knowledge of the extremal's position has
been accumulated by the preceding portion of the search and the
problem involves a smooth function. The global search can be
used to advantage in the *opening moves* of a search. In the
early phase of a search the object is to isolate the approx-
imate neighborhood of the minimum performance function
value as rapidly as possible, usually with little or no
foreknowledge of the performance function behavior. One
measure of the effectiveness of a search algorithm in such

a situation is the number of evaluations required to locate the minimum point to some prespecified accuracy. It can be shown that the most effective method of locating the minimum point of a general unimodal function is a *Fibonacci search*, reference 4. In this method, the accuracy to which the minimum is to be located along the perturbation parameter axis must be selected prior to the commencement of the search. Since the accuracy required is highly dependent on the behavior of the performance function, this quantity is difficult to prespecify.

Prespecification of the accuracy to which the extremal's position is to be located can be avoided for little loss in search efficiency by use of an alternative search based on the so-called golden section, reference 8. This is the method employed in the AESOP code one-dimensional search procedure. Search by the golden section commences with the evaluation of the performance function at each end of the search interval and at $G = 2/(1 + \sqrt{5}) = .6180339887$ of the interval from both of these bounding points. This is illustrated in Figure 1.

The boundary point furthest from the lowest resulting performance function value is discarded. The three remaining points are retained, and the search continues in a region which is diminished in size by G. The internal point at which the performance function is known in the reduced interval will be at a distance G of the reduced interval from the remaining bounding point of the original interval for $(1 - G) = G^2$. The search can, therefore, be continued in the reduced interval with a single additional evaluation of the performance function. It follows after Q evaluations of the performance function that the position of the extremal point will be known to within R of the original search region
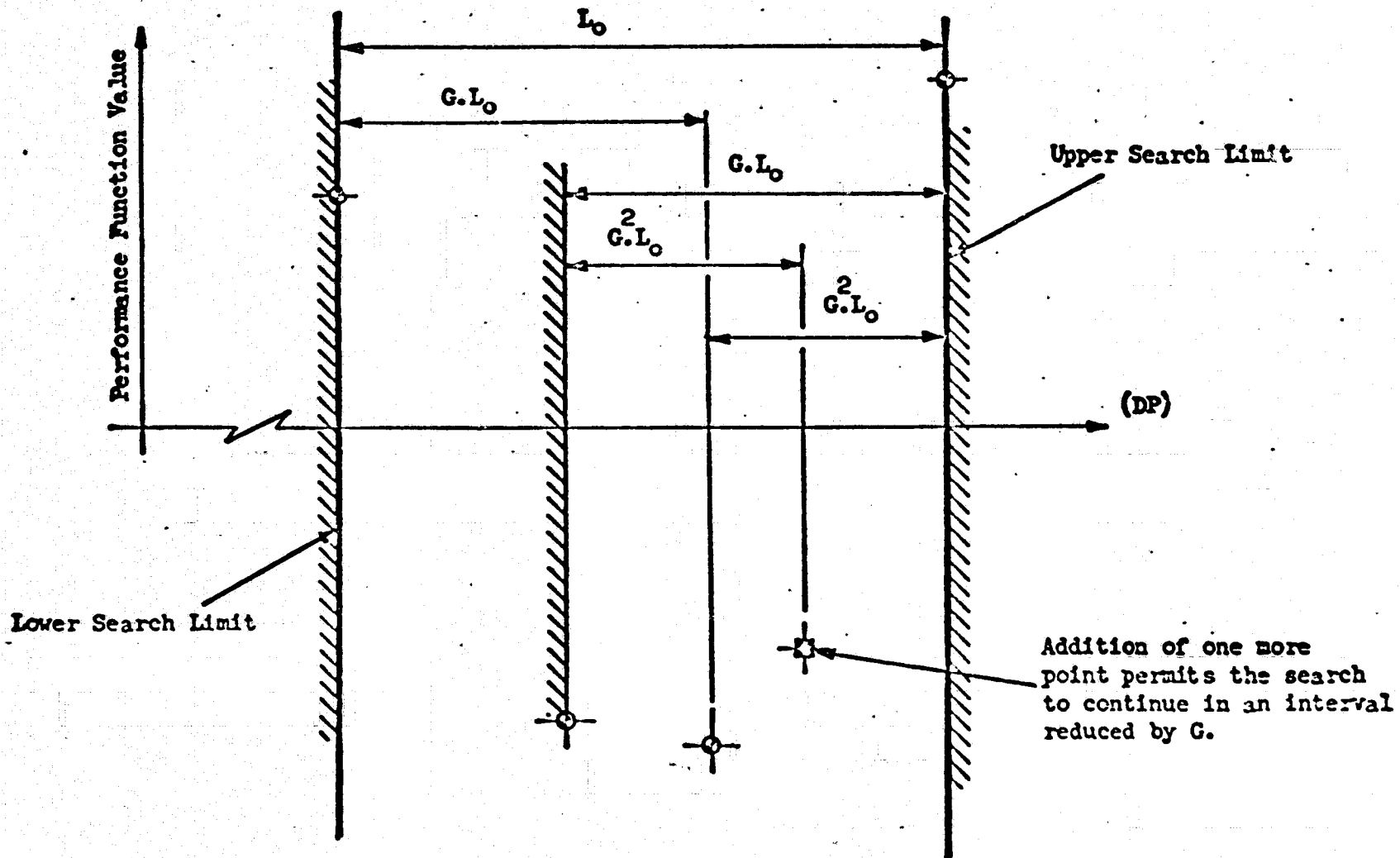
FIGURE 1. SEARCH BASED ON THE GOLDEN SECTION

where

$$R = G^{(Q-3)} \qquad\qquad (9)$$

To reduce the interval of uncertainty to .00001 of
the original search interval, about 27 evaluations of the
performance function are required. For a reasonable number
of evaluations of the performance function this type of
search is almost as efficient as a Fibonacci search.

It should be noted that search by the golden section
proceeds under the assumption of unimodality; hence, it will
often fail to detect the presence of more than one minimum
when the performance function is multimodal. If more than
one minimum does exist, the one located depends on perfor-
mance function behavior within the original search interval.

Multiple Extremals on One-Dimensional Ray. The one-
dimensional section search described above is unable to
distinguish one local extremal from another; it will merely
find one local extremal. This difficulty can be largely
eliminated by the addition of some logic to the search, at
least for moderately well behaved performance functions;
that is, for functions having a limited number of extremals
in the control space region of interest. An effective method
for detecting multiple extremals is to combine the one-
dimensional search with a random one-dimensional search on
the same ray through the control space. This is illustrated
in figures 2 and 3. In figure 2 the response contours of
a performance function having two minima are illustrated
together with the initial points used in a global one-
dimensional search by the golden section method. The
behavior of the function at these points is shown in
figure 3. The left hand minimum is not apparent from
these points. If a single random point is added in the
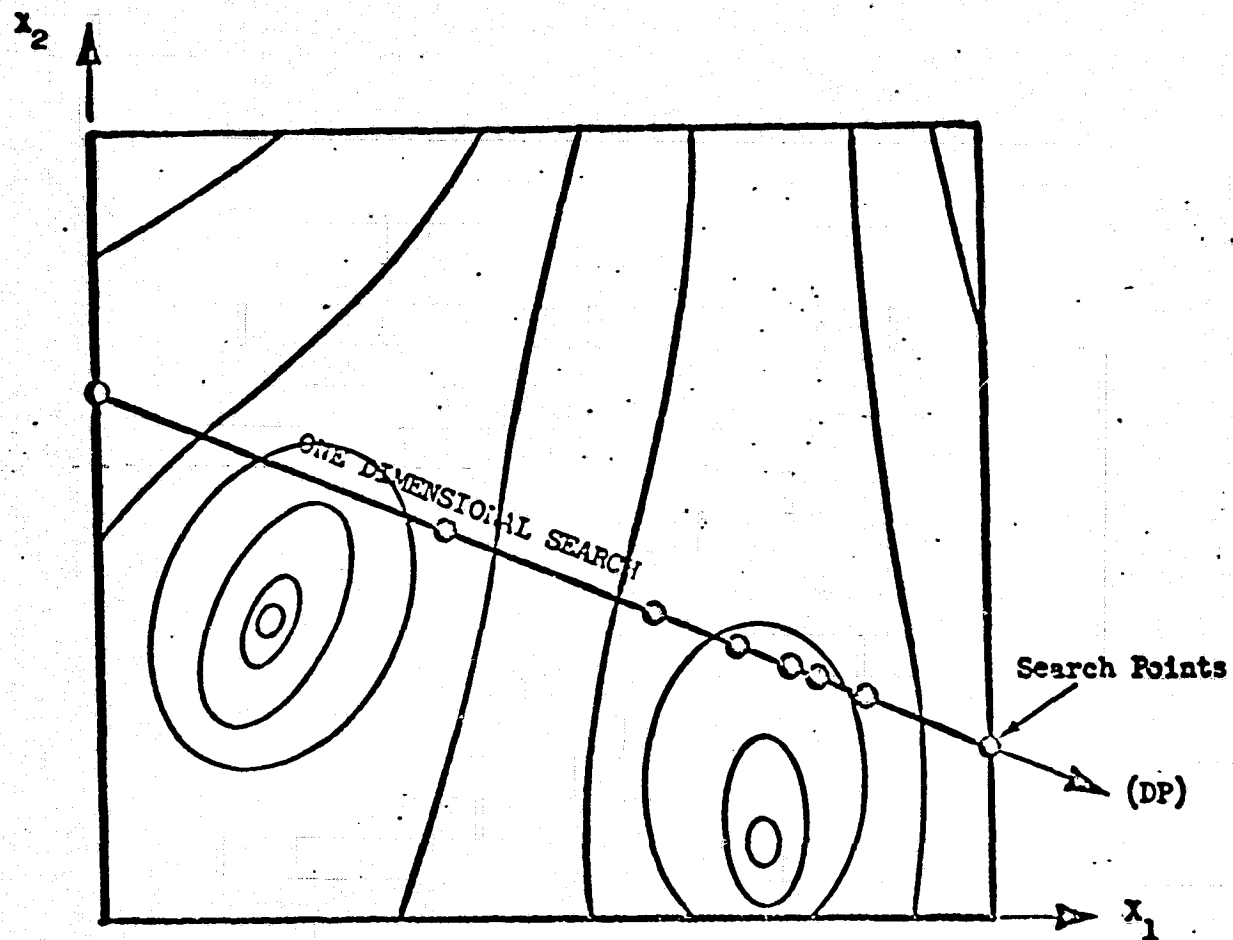interval L_0, the probability of this point revealing the

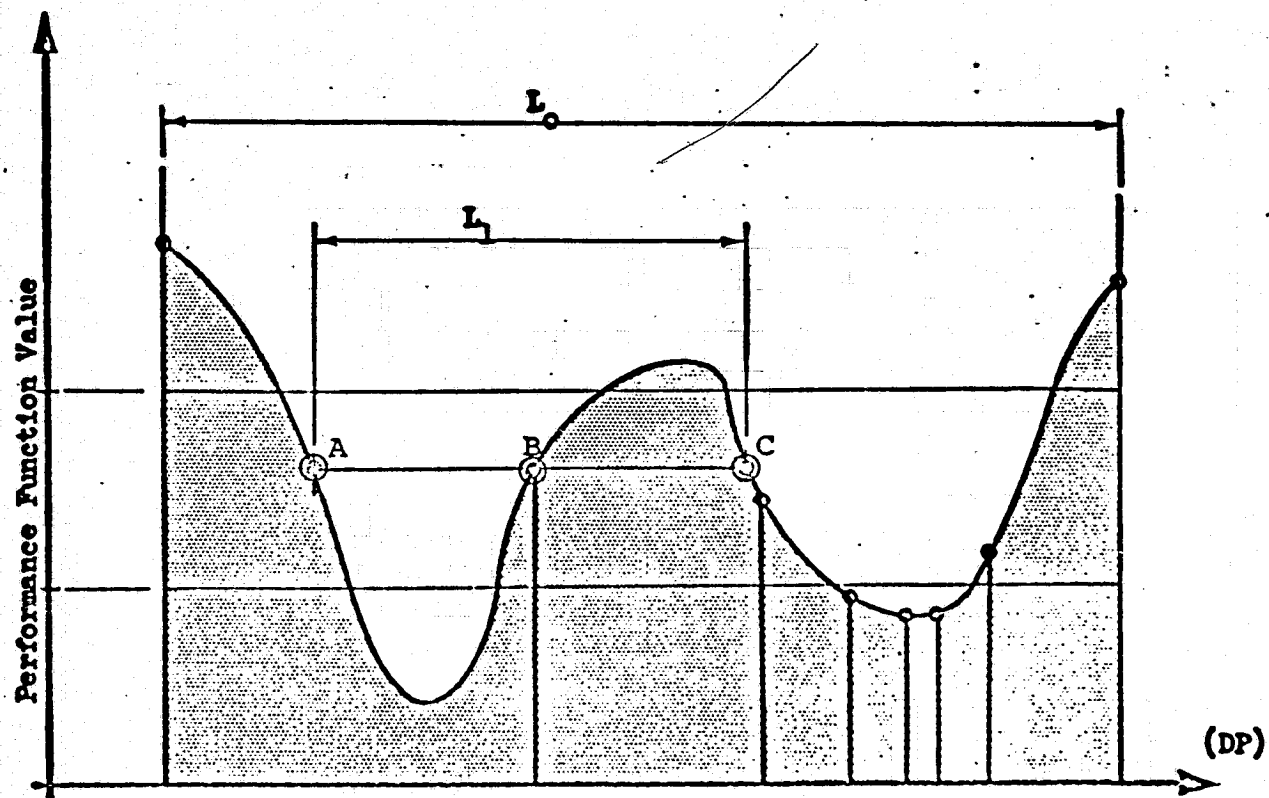FIGURE 2. RESPONSE SURFACE WITH TWO TROUGHS

FIGURE 3. SEARCH BY GOLDEN SECTION FAILS TO DETECT MULTIPLE TROUGHS ON ONE DIMENSIONAL CUT

presence of the second minimum is

$$P_1 = L_1/L_0 \qquad\qquad (10)$$

for any point in the interval AB indicates the presence of
a local minimum somewhere in the interval AB, and any point
in the interval BC indicates the presence of a local maximum
somewhere in the interval BC. In this latter case, there
must be a minimum of the function both to the left and to the
right of the newly introduced point.

If R random uniformly distributed points are added in the
interval L_0, the probability of locating the presence of
the second minimum becomes

$$P_R = 1.0 - (1.0 - L_1/L_0)^R \qquad\qquad (11)$$

The function (L_1/L_0) is a measure of the performance
function behavior. For a given value of this behavior function
the number of random points which must be added to the one-
dimensional search to provide a given probability of locating
a second minimum can be determined.

The presence of multiple minima on a one-dimensional cut
through an N-dimensional space does not necessarily indicate
that the performance function possesses more than one minimum
in a multi-dimensional sense. It may be that the performance
function is merely non-convex. This is illustrated by figure
4. The performance function behavior on the one-dimensional
search in figures 2 and 4 is identical. In figure 2 this
indicates the presence of two local extremals; in figure 4,
a non-convex performance function.

When a one-dimensional search detects the presence of
multiple extremals in the local sense above, a decision must

be made as to which of the apparent extremals is to be pursued during the remainder of the search. Here, without foreknowledge of the performance function behavior, logic must suffice. Typically, the left or right hand extremal, the extremal which results in the best performance, or even a random choice may be made.

It should be noted that logic of this type is not currently available in the AESOP code. The AESOP one-dimensional search procedure has three distinctive phases. *First*, each search algorithm defines an initial perturbation using either past perturbation stepsize information or a perturbation magnitude prediction as in the quadratic search below. *Second*, a perturbation stepsize doubling procedure is employed until a point exhibiting diminishing performance is generated. *Third*, having coarsely defined the one-dimensional extremal position from steps one and/or two, a golden section search is employed to locate the extremal with reasonable precision.

Multiple extremals - general procedure. The multiple extremal search technique included in AESOP is based on *topologically invariant warping* of the performance response surface. The response surface is warped in a manner which retains all the surface extremals but alters their relative locations and *regions of influence*. The region of influence of an extremal is defined as the hull or collection of all points which lead to the extremal if a gradient path is followed. Reducing the region of influence of an extremal

PRECEDING PAGE BLANK NOT FILMED

14
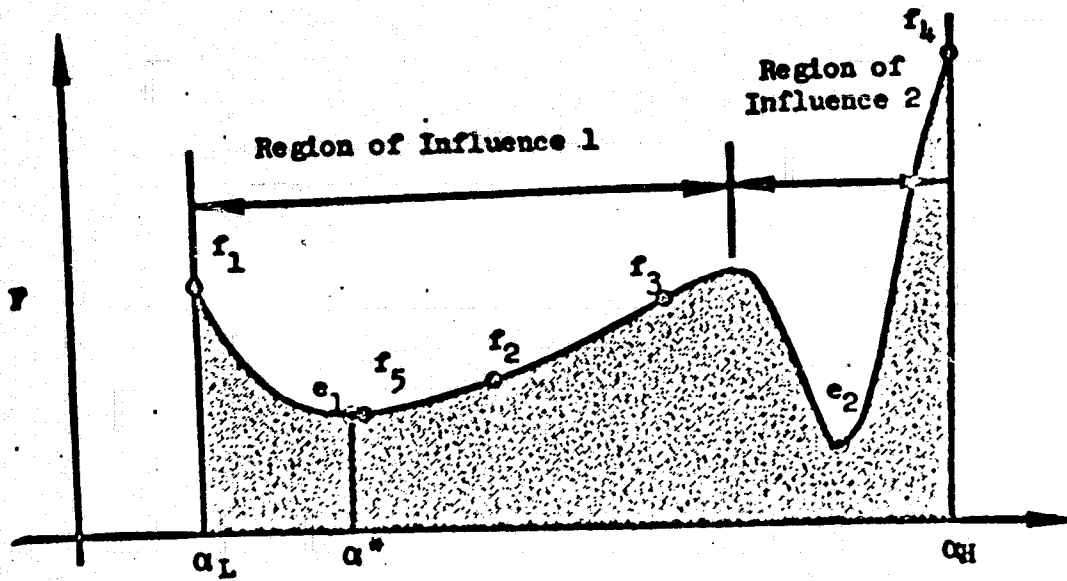
FIGURE 5. FUNCTION WITH TWO EXTREMALS

decreases the *probability* of locating a point in the neighborhood of the extremal if points are chosen at random. Again, in an organized multivariable search, the probability of locating an extremal having a small region of influence is less than that of locating an extremal having a large region of influence. For example, suppose the extremals of the one-dimensional function of figure 5 are to be determined in the range $\alpha_L < \alpha < \alpha_H$ by the sectioning approach. The four initial values employed in this technique are denoted by f_1 to f_4.

Following evaluation at these four points, f_4 is discarded, and the function is evaluated at f_5. At this point the right-hand extremal, e_2, has been eliminated from the search which now inevitably proceeds to the left hand extremal at e_1.

To find the second extremal, the Function F is warped by writing

$$F(\xi) = F(\alpha) \quad \quad \quad (12)$$

16

$$\xi = (\alpha_H - \alpha^*)\left[\frac{\alpha - \alpha^*}{\alpha_H - \alpha^*}\right]^{2N} + \alpha^*; \quad \alpha > \alpha^*$$

$$\xi = -(\alpha^* - \alpha_L)\left[\frac{\alpha^* - \alpha}{\alpha^* - \alpha_L}\right]^{2N} + \alpha^*; \quad \alpha^* > \alpha \qquad (13)$$

where N is a positive integer, and α^* is the location of the left hand extremal.

A typical relationship between ξ and α is shown in figure 6 for the case N = 1. Differentiation of equation (13) with respect to α when N = 1 results in

$$\xi' = \frac{2[\alpha - \alpha^*]}{[\alpha_H - \alpha^*]}; \quad \alpha \geqslant \alpha^*$$

$$\xi' = \frac{2[\alpha^* - \alpha]}{[\alpha^* - \alpha_L]}; \quad \alpha < \alpha \qquad (14)$$

Note that as $\alpha \to \alpha^*$, $\xi' \to 0$ from both the left and right. At $\alpha = \alpha_L$ and at $\alpha = \alpha_H$, $\xi' = 2$. In the regions $\alpha_L < \alpha < \alpha^*$ and $\alpha^* < \alpha < \alpha_H$, ξ varies parabolically with α. Figure 6 illustrates these points. It can be seen that a region $\Delta\alpha_1$ centered about α^* transforms into a smaller region $\Delta\xi_1$ located in the neighborhood of $\xi = \alpha^*$. On the other hand, a region $\Delta\alpha_2$ situated in the

17

neighborhood of the upper search limit, α_H, maps into a wider region in the neighborhood of $\xi = \alpha_H$. In general, the slopes at $\alpha = \alpha_L$ and $\alpha = \alpha_H$ are given by 2N; the greater N, the greater the warping becomes.

The effect of introducing a moderate warping transformation on the function of figure 5 is shown in figure 7. It can be seen from figure 7 that the region of influence of e_1 is reduced, and the region of influence of e_2 is increased. On the warped surface search by sectioning commences with evaluations of performance at f_1' to f_4'. Following these initial evaluations f_1' is discarded (as opposed to the discard of f_4 on the unwarped surface), and the function is evaluated at the additional point f_5'. The points f_3' and f_5' straddle the extremal e_2 which is now inevitably located by further sectioning evaluations. Figures 8a and 8b illustrate the warping transformations for N = 1 and N = 10 when the transformation is applied at the point $a^* = .5$, the symmetric case. It can be seen that when N = 1, twenty per cent of the warped control space corresponds to approximately 45 per cent of the unwarped control space in the vicinity of the transformation origin ($\alpha = .5$). When N = 10 twenty per cent of the warped control space transforms into ninety per cent of the unwarped control space.

Sectioning Parallel to the Axes. The independent variable perturbation algorithm in the sectioning search is

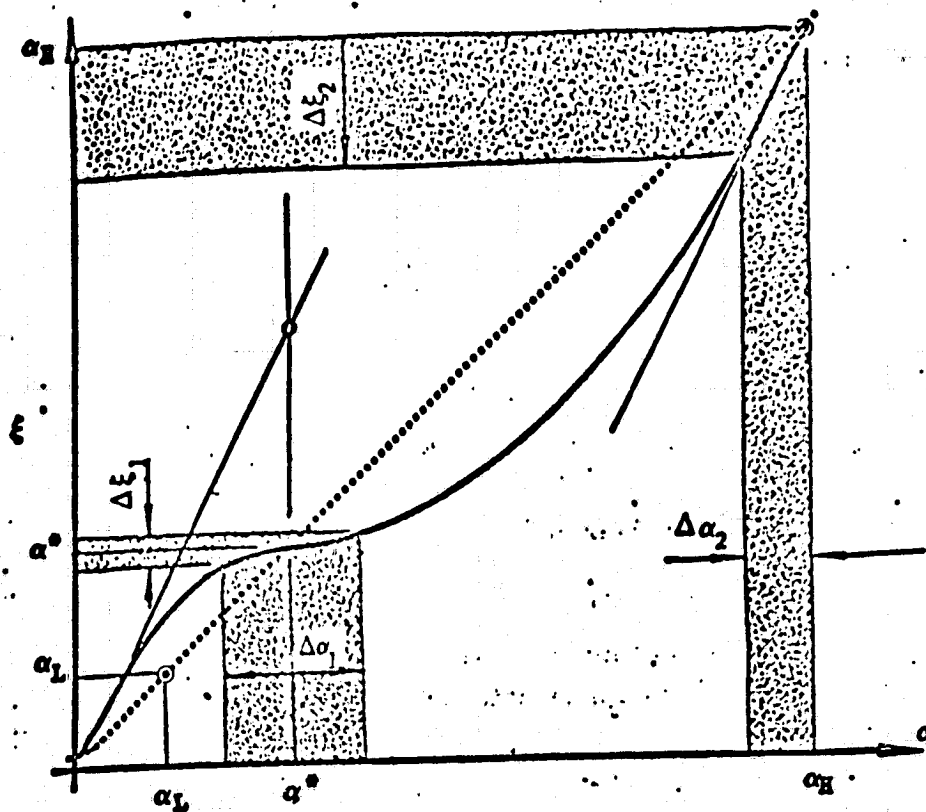$$\Delta\alpha_i = 0, \quad i \neq r$$
$$= DP, \quad i = r \quad r = 1, 2, \ldots, N \quad (15)$$

18

FIGURE 6. WARPING TRANSFORMATION
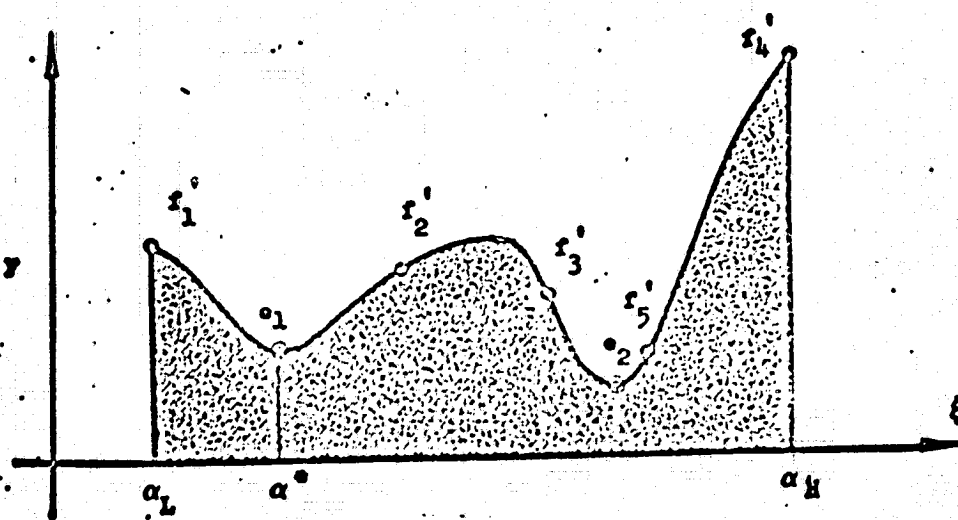
FIGURE 7. TRANSFORMED FUNCTION WITH TWO
EXTREMALS

WARPN = 1 (WARPING TRANSFORMATION ALPHA* = 0.5)

1.00
.90
.80
.70
.60
.50
.40
.30
.20
.10
0

.10 .20 .30 .40 .50 .60 .70 .80 .90 1.00
ALREAL

WARPN = 2 (WARPING TRANSFORMATION ALPHA* = 0.5)

1.00
.90
.80
.70
.60
.50
.40
.30
.20
.10
0

ALPHA

.10 .20 .30 .40 .50 .60 .70 .80 .90 1.00
ALREAL

WARPN=3 (WARPING TRANSFORMATION ALPHA* = 0.5)

1.00
.90
.80
.70
.60
.50
.40
.30
.20
.10
0

.10 .20 .30 .40 .50 .60 .70 .80 .90 1.00
ALREAL

WARPN=4 (WARPING TRANSFORMATION ALPHA* = 0.5)

1.00
.90
.80
.70
.60
.50
.40
.30
.20
.10
0

ALPHA

.10 .20 .30 .40 .50 .60 .70 .80 .90 1.00
ALREAL

FIGURES 8(a) to 8(d).   WARPING TRANSFORMATION N = 1 to 4

20
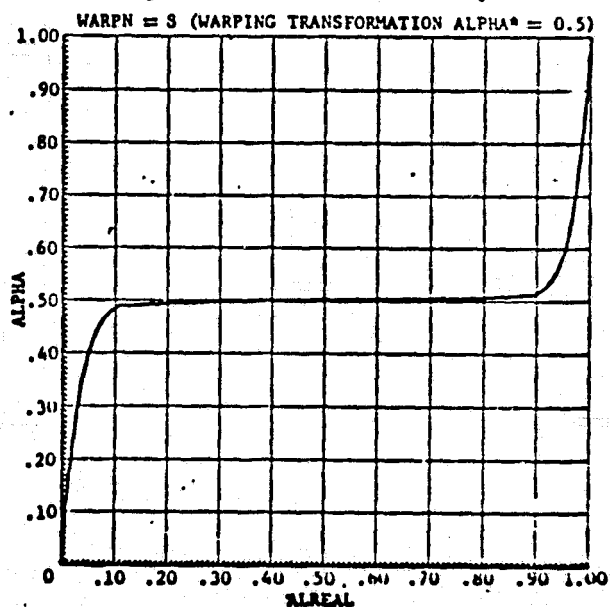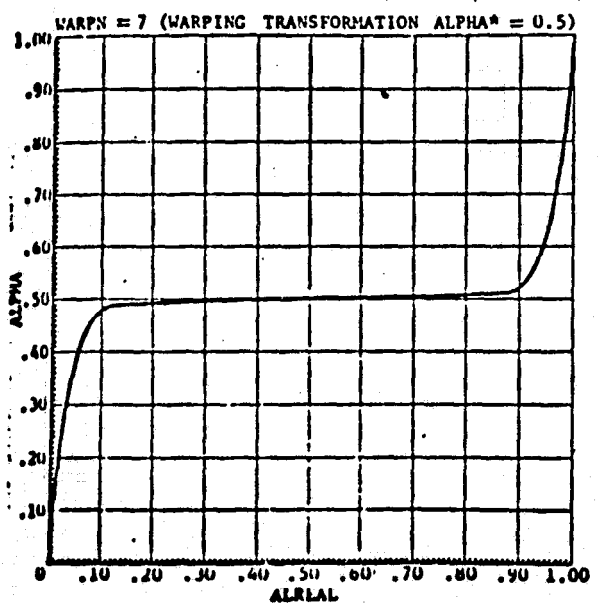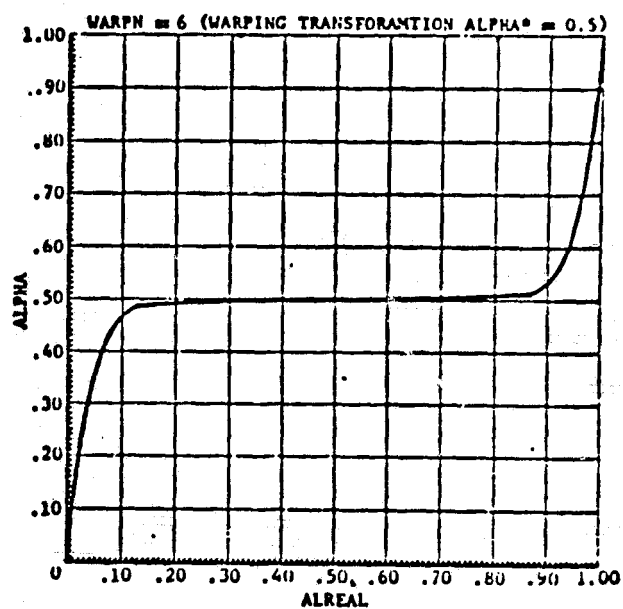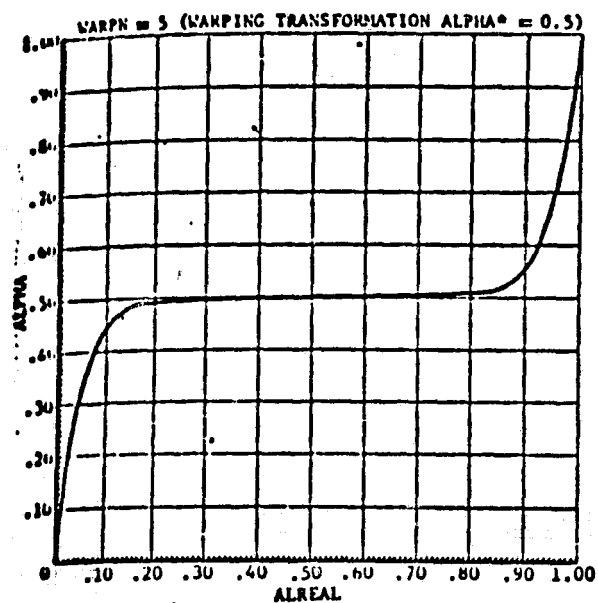
FIGURES 8(e) to 8(h).   WARPING TRANSFORMATION N = 5 to 8

WARPN = 10 (WARPING TRANSFORMATION ALPHA* = 0.5)

WARPN = 9 (WARPING TRANSFORMATION ALPHA* = 0.5)
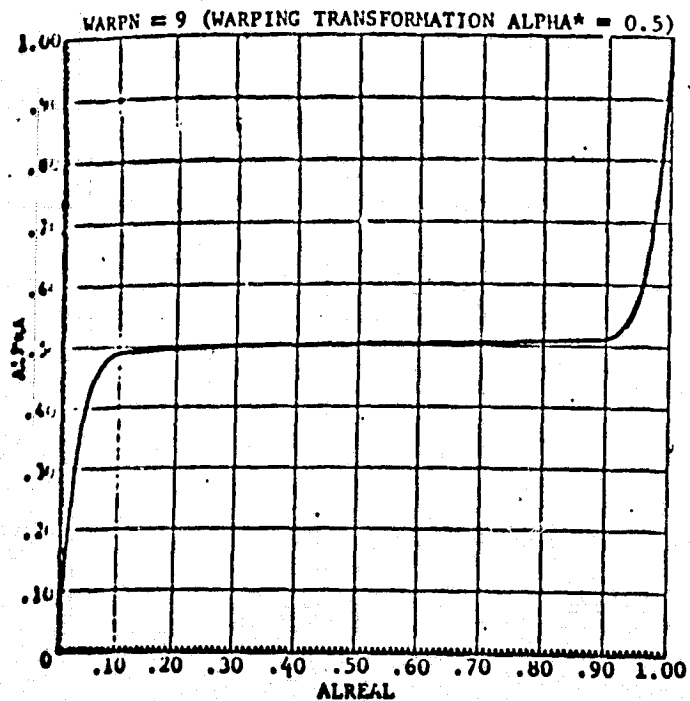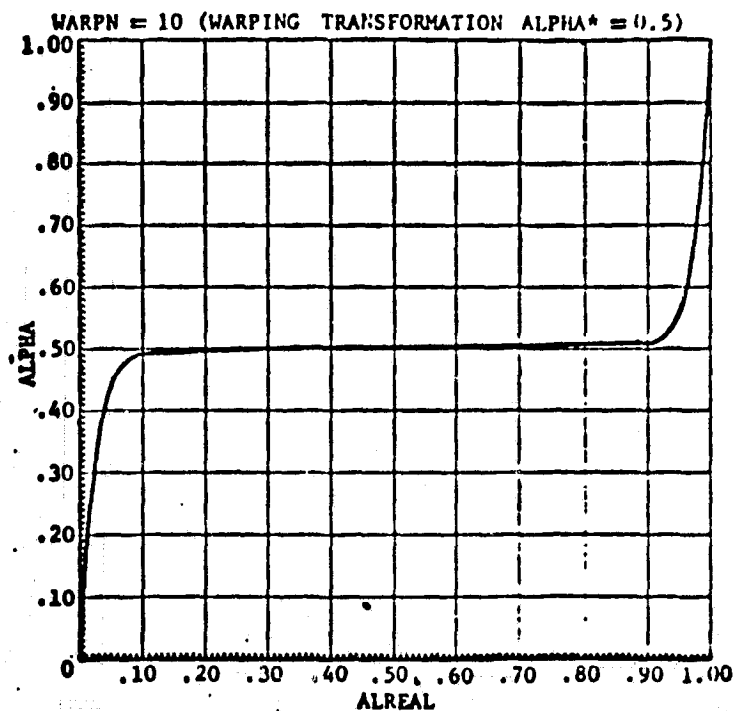
FIGURES 8(i) and 8(j). WARPING TRANSFORMATION N = 9 and 10

22

This is simply the parametric or univariate search approach. All but one of the independent variables are held constant while a one-dimensional search parallel to the Rth variable axis determines the best value of the remaining variable, α_r. The variable α_r is then *set to this value,* and the process is repeated with one of the remaining independent variables. When all N independent variables have been perturbed in this way, a sectioning search cycle has been completed.

The N-dimensional search can then be continued with another cycle of sectioning or by one of the other search techniques described below. In practice, it has been found advantageous to *perturb the independent variables in a random order* within each sectioning cycle. The method can be used in conjunction with either a local or a global search as outlined in the two preceding sections. The behavior of this search in the solution of a straightforward two-variable optimization problem is illustrated in Figure 9. It may be noted that the AESOP code searches from boundary to boundary in each variable using a golden section search procedure.

Sectioning to Define Local Sensitivities. The sectioning search can readily be applied to the problem of performance or constraint sensitivity determination. Thus, by the device of omitting the updating of each control variable α_r following the sectioning search on the rth parameter, the sequence of sectioning searches is performed about a fixed nominal point. When such a search is performed in the vicinity of a known extremal point, the penalties for off-optimal design can be assessed. Away from an extremal point, the search merely provides local sensitivities in a similar manner to the manual perturbation methods employed in *conventional trial and error* design evolution.

23
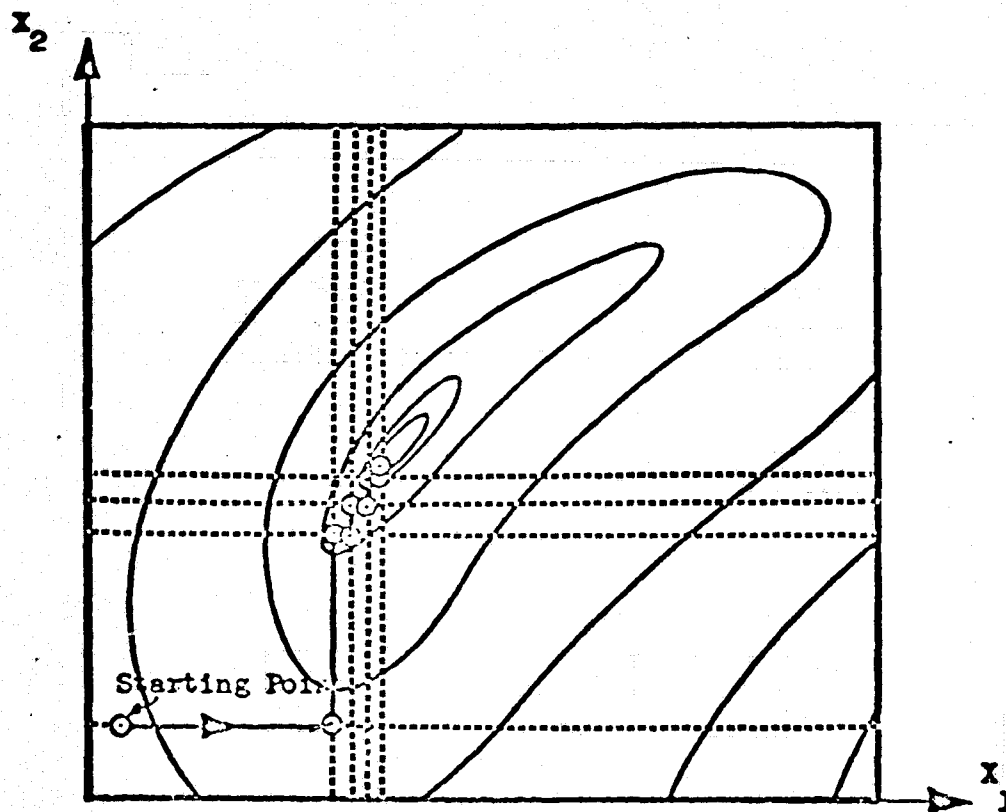
FIGURE 9. SECTIONING PARALLEL TO THE AXES

Steepest-Descent Search. The steepest-descent search
algorithm is

$$\{\Delta\alpha\} = -[W]^{-1}\left\{\{\frac{\partial\phi}{\partial\alpha}\} - [\frac{\partial C}{\partial\alpha}]^T[K_3]^{-1}\{K_2\}\right\}$$

$$\times \sqrt{\frac{(DP)^2 - DC\ [K_3]^{-1}\{DC\}}{K_1 - K_2\ [K_3]^{-1}\{K_2\}}}$$

$$- [W]^{-1}\ [\frac{\partial C}{\partial\alpha}]^T\ [K_3]^{-1}\ \{DC\} \qquad (16)$$

Here, the *matrix W is the metric tensor* of the control space
and serves to define a generalized measure for the *magnitude*
of a control vector perturbation. The vectors $\{\partial\phi/\partial\alpha\}$ and
$\{\partial C/\partial\alpha\}$ are defined as

$$\left\{\frac{\partial\phi}{\partial\alpha_1}\ ,\ \frac{\partial\phi}{\partial\alpha_2},\ \cdot\ \cdot\ \cdot\ \frac{\partial\phi}{\partial\alpha_n}\right\}$$

and

$$\left\{\frac{\partial C}{\partial\alpha_1}\ ,\ \frac{\partial C}{\partial\alpha_2}\ ,\ \cdot\ \cdot\ \cdot\ \frac{\partial C}{\partial\alpha_n}\right\}$$

respectively. The K matrices are defined as

$$K_1 = \lfloor\frac{\partial\phi}{\partial\alpha}\rfloor\ [W]^{-1}\ \{\frac{\partial\phi}{\partial\alpha}\} \qquad (17)$$

$$\{K_2\} = [\frac{\partial C}{\partial\alpha}][W]^{-1}\{\frac{\partial\phi}{\partial\alpha}\} \qquad (18)$$

$$[K_3] = [\frac{\partial C}{\partial\alpha}][W]^{-1}\ [\frac{\partial C}{\partial\alpha}]^T \qquad (19)$$

The perturbation parameter, (DP), is defined by

$$(DP) = \lfloor \Delta\alpha \rfloor [W]\{\Delta\alpha\} \tag{20}$$

The vector $\overline{DC}$ is the *desired change in the constraint functions*. For an unconstrained problem, (16) reduces to

$$\{\Delta\alpha\} = -[W]^{-1}\{\frac{\partial\phi}{\partial\alpha}\}\sqrt{\frac{(DP)^2}{K_1}} \tag{21}$$

The performance function change associated with the perturbation of equation (16) is

$$D\phi = -\left(K_1 - \lfloor K_2 \rfloor [K_3]^{-1}\{K_2\}\right)^{.5}\left((DP)^2 - \lfloor DC \rfloor [K_3]^{-1}\{DC\}\right)^{.5}$$

$$+ \lfloor K_2 \rfloor [K_3]^{-1}\{DC\} \tag{22}$$

Equation (16) does not specify a one-dimensional search directly since the perturbation parameter (DP) and each component of the constraint vector change $\overline{DC}$ can be independently specified. This difficulty is conveniently eliminated if the components of $\overline{DC}$ are expressed in terms of the perturbation parameter. Let (DP) and $\overline{DC}$ be arbitrarily assigned, say (DP_0) and $\overline{DC}_0$, respectively. Now consider the one parameter set of values for $\overline{DC}$ defined by

$$\overline{DC} = \left(\frac{DP}{DP_0}\right) \cdot \overline{DC}_0 \tag{23}$$

It follows from equations (16) and (22) that (23) specifies a one parameter family of perturbations in which the non-linear performance and constraint functions *vary linearly with (DP)*, to the first order.

Equations (16) to (22) are valid for small perturbations in the independent variables provided the derivatives involved are *continuous in the region of the control space* defined by equation (20). In practice, when this condition is not satisfied, the steepest-descent algorithm can be used to locate a promising direction for a one-dimensional search provided the derivatives are computed numerically. In this case, however, equation (22) ceases to provide an accurate indication of performance function behavior along the specified ray.

When dealing with performance and constraint functions having continuous first derivatives, the perturbation parameter value to be used in equation (16) can be determined from a second order Taylor's expansion of the performance function behavior in terms of DP. The coefficients in this series expansion can be readily obtained from the conditions of zero change for DP = 0, linear slope for DP = 0, and from the actual value of the performance function at a point in the neighborhood of the point at DP = 0. This method for determining the best perturbation parameter value is discussed in some detail in references 5 and 6. When dealing with less regular functions, the one-dimensional search by sectioning can be used to determine the perturbation parameter value. This is the technique employed in the optimization program, AESOP, references 1 and 2; for the AESOP code converts all

constrained optimization problems to unconstrained problems by the penalty function device, equation (6). The resulting response surface combines both performance function and weighted constraint functions. Inevitably, this surface has a more complex topology than that of the unconstrained performance function. Program AESOP is also limited to the penalty function approach to constrained optimization, and, hence, it utilizes the reduced algorithm of equation (21) rather than the explicit constraint algorithm of equation (16).

Steepest-Descent Weighting Matrices. The weighting matrix introduced in equations (16) and (20) must be *positive definite* to assure a positive distance between any two non-coincident points in the control space. Apart from this restriction, the choice of weighting matrix is arbitrary. Inspection of equation (16) reveals that any descending direction is a steepest-descent path for some choice of the weighting matrix W. This can be simply illustrated when only two independent variables are involved. Figure 10 depicts a small region of the control space R^2. The performance function response contours appear as a series of parallel lines on this microscopic region of the control space. The perturbation zones corresponding to three weighting matrix choices are shown. The first zone corresponds to the choice of a unit matrix for W. It follows from equation (20) that for a given value of $(DP)^2$ the search zone is a circle of radius (DP). The steepest-descent direction is that in which the performance improvement is greatest. This is the direction of a line from the origin

of the circular search zone to that point on its circumference which provides the smallest value of the performance function $\phi(\bar{a})$. With this choice of weighting matrix, the steepest-descent direction is perpendicular to the response contours. Paths of this type are illustrated in figure 11 by the solid lines emanating from points A and B. From the nominal point A, search perpendicular to the performance response contours is very efficient. From point B, however, this type of search results in the meandering path illustrated. It is assumed here that once a steepest-descent direction is located, an exhaustive search for the minimum in that direction will be undertaken in view of the high cost of recomputing the derivatives in many problems. Even if this were not the case, search normal to the response contours can often be improved upon. For example, it is obvious that even in the straightforward two-dimensional problem of figure 11 the dashed search direction is superior. This direction requires *a priori* knowledge of the extremal's position, information not normally available.

Returning to figure 10, the second search zone depicted corresponds to the choice of a diagonal matrix for W. The positive-definite constraint on W requires that all diagonal elements of the weighting matrix be positive. In this case the search zone becomes elliptical with the major and minor axes of the ellipse being parallel to the coordinate axes. It may be noted that as either of the diagonal elements of W becomes large in relation to the remaining element, the corresponding element in W inverse together with the predicted change in the associated independent variable becomes small. In the limit this reduces the search to a one-dimensional search in the remaining coordinate. The perturbation zone then becomes a slit
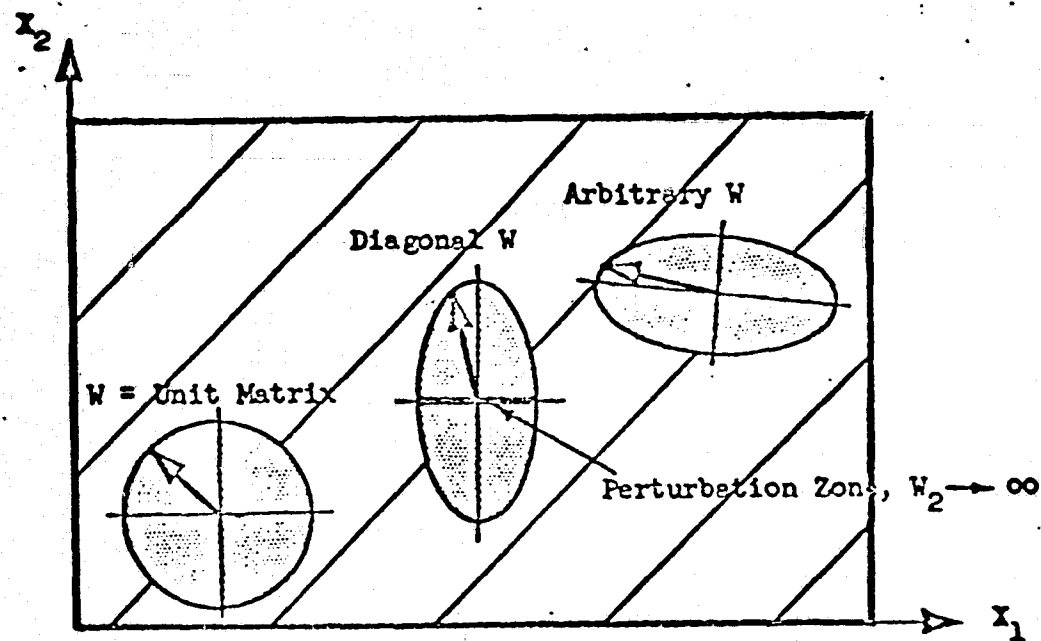
FIGURE 10.-PERTURBATION ZONES CORRESPONDING
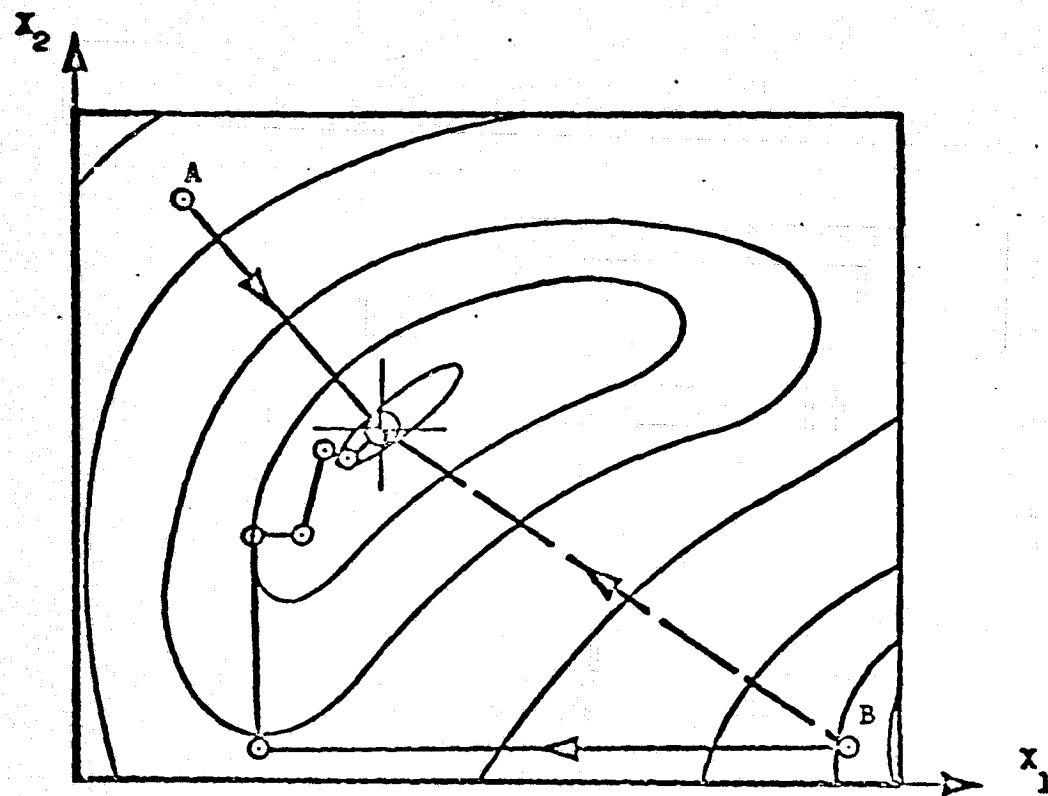TO THREE WEIGHTING MATRICES

FIGURE 11.-STEEPEST-DESCENT SEARCH

parallel to that coordinate axis of length 2 · (DP), as illustrated in figure 10. In the case illustrated, the steepest-descent path is in the descending α_1 direction.

Finally, the search zone corresponding to the choice of an arbitrary positive-definite weighting matrix is shown. From equation (20) and the positive-definite constraint on W, the search zone remains elliptical, but the principle axes may now have an arbitrary orientation to the axes of α_1 and α_2. It follows that since the elliptic search zone can have any orientation and eccentricity, *any direction in the control space is a possible steepest-descent path;* for in all cases, the path of steepest-descent lies in the direction of a line joining the search zone origin to the lower point of tangency between the boundary of the search zone and the performance function response contours. The discussion above may readily be extended to control spaces of higher dimensionality.

When attempting the solution of optimization problems by the steepest-descent method, the analyst is constantly faced with the problem of choosing a satisfactory weighting matrix for the search continuation. The problem is compounded by the fact that the slopes of the performance function with respect to the independent variables can, and frequently do, vary by many orders of magnitude. The arbitrary choice of a unit matrix in such situations can lead to distressingly slow convergence of the numerical search; for it is in the nature of many problems that in those directions in which *the slopes are greatest the response surface is highly non-linear.* Only small perturbations will be successful in the direction of these strong control variables. In those directions in which the slopes are small, the contours are often relatively linear, and *large perturbations may be required in these weak control variables.*

In such situations the local steepest-descent direction for (W) = (I) is misleading. With this choice of weighting matrix perturbations are in proportion to the response surface partial derivatives. However, the best direction in which to proceed may involve large perturbations in the weak control variables of small slope. This behavior is illustrated for a two-dimensional case in figure 11 by the dashed line emanating from B.

The problem of choosing a satisfactory weighting matrix also arises when the steepest-descent search is applied in its variational form, reference 5, and when a combination of continuous control variables and parameters are encountered as in the optimization of multiple-arc problems in flight path optimization problems, reference 6. In these references it is suggested that the weighting matrices be based on the *first derivatives* of the unconstrained performance function with respect to the control. This approach can be used in the solution of multivariable optimization problems also, by writing

$$W_{ij}^{-1} = A_i + B_i \left| \frac{\partial \phi}{\partial \alpha_j} \right| , \quad i = j$$

$$= 0, \quad i \neq j$$

In practice, alternate use of the resulting combined weighting matrix and the unit matrix tends to provide a reasonable convergence rate at points well removed from the extremal. The AESOP code employs such a matrix in combination with a search range non-dimensionalization term and a learning factor. The learning factor emphasizes perturbation of control parameters which change in a monotonic direction and de-emphasizes those perturbations which fluctuate in sign.

Random Ray Search. The difficulty of defining a suitable control variable metric tensor together with

the fact that any descending path is a steepest-descent direction for some choice of metric tensor suggests the possibility of searching along a random ray through the control space. The algorithm for random ray search is

$$\Delta\alpha_i = R_i(\pm DP), \quad i = 1, 2, \ldots, N \quad (25)$$

where the R_i, proportional to the direction cosines of the ray, are uniformly distributed random numbers satisfying

$$-1.0 < R_i < +1.0, \quad i = 1, 2, \ldots, N$$

The positive sign in equation (25) is taken if $\frac{d\phi}{d(DP)}$ is negative; the negative sign is taken when this derivative is positive. The method is equivalent to a steepest-descent search *using a randomly generated metric tensor.*

Quadratic search[*]. An alternative systematic approach to the definition of an arbitrary or empirical weighting matrix is provided by second order or quadratic method. It can be shown, for example, in reference 1, that on an elliptic second order response surface the weighting matrix

$$W_{ij} = \left(\frac{\partial^2 \phi}{\partial\alpha_i \partial\alpha_j}\right) \quad (26)$$

when used in the steepest-descent method will immediately define the optimal point

$$\{\alpha^*\} = \{\alpha_0\} + \{\delta\alpha\} \quad (27)$$

* Also known as the Newton-Raphson method

34

where $\{\delta\alpha\}$ is computed from equation (21) with $(DP)^2 = .5K_1$. On a more general non-linear response surface, equation (27) merely defines a direction for subsequent search in the manner of the steepest-descent technique. This is illustrated in figure 12. Here, the approximating elliptical contours computed at point 0 define an approximate extremal location at P through equations (26) and (27). Subsequent search along the ray OP results in the definition of a one-dimensional extremal. This point is then used to fit another approximating elliptic contour, and the process is repeated until the extremal point at Q is located.

The quadratic search procedure can be quite rapid in control spaces of low dimensionality. In high order spaces the approach is usually impractical as a result of the requirement to establish the second order weighting matrix of equation (26). In many practical engineering problems these derivatives cannot be obtained in closed form; in such cases the derivatives must be obtained numerically, for example, reference 1. Computation of these derivatives requires at least $(N+1)(N+2)/2$ evaluations of ϕ at each point where an approximating quadratic is employed. Clearly, for large N this computation may become impractical in computational time.

Davidon or Fletcher-Powell Method. Davidon's method is a hybrid first order/second order technique. The objective of Davidon's method is to arrive at a reasonable approximation to the second order weighting matrix of equation (26) without the use of $(N+1)(N+2)/2$ evaluations of ϕ. It can be shown that on a quadratic (second order) response surface N steepest-descent searches performed in
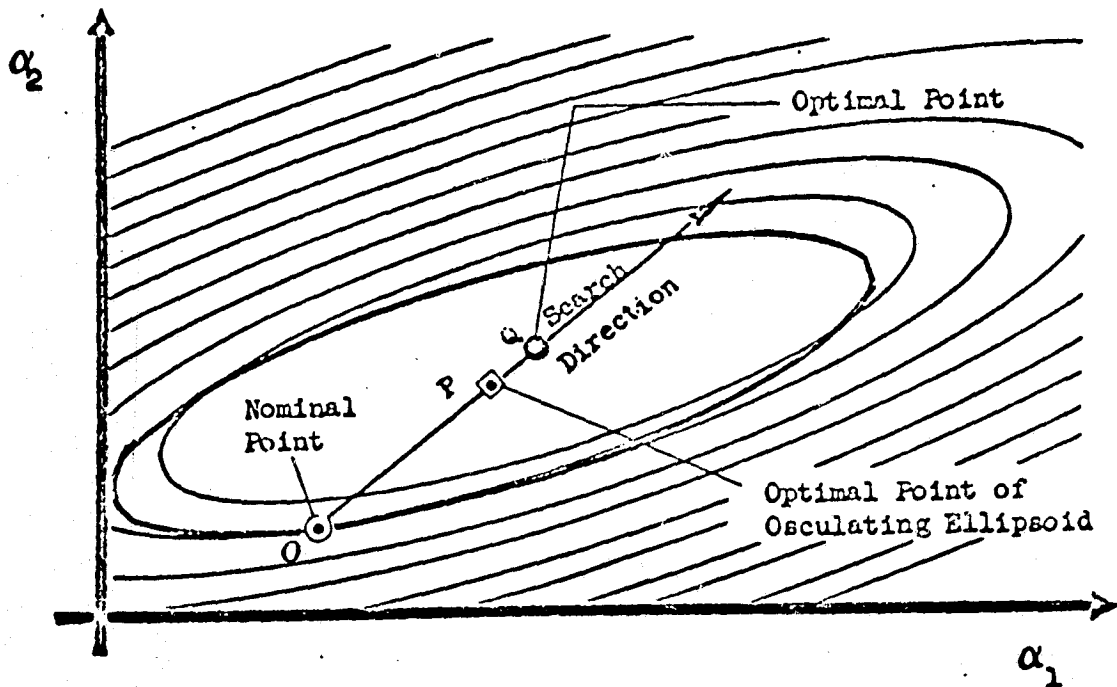
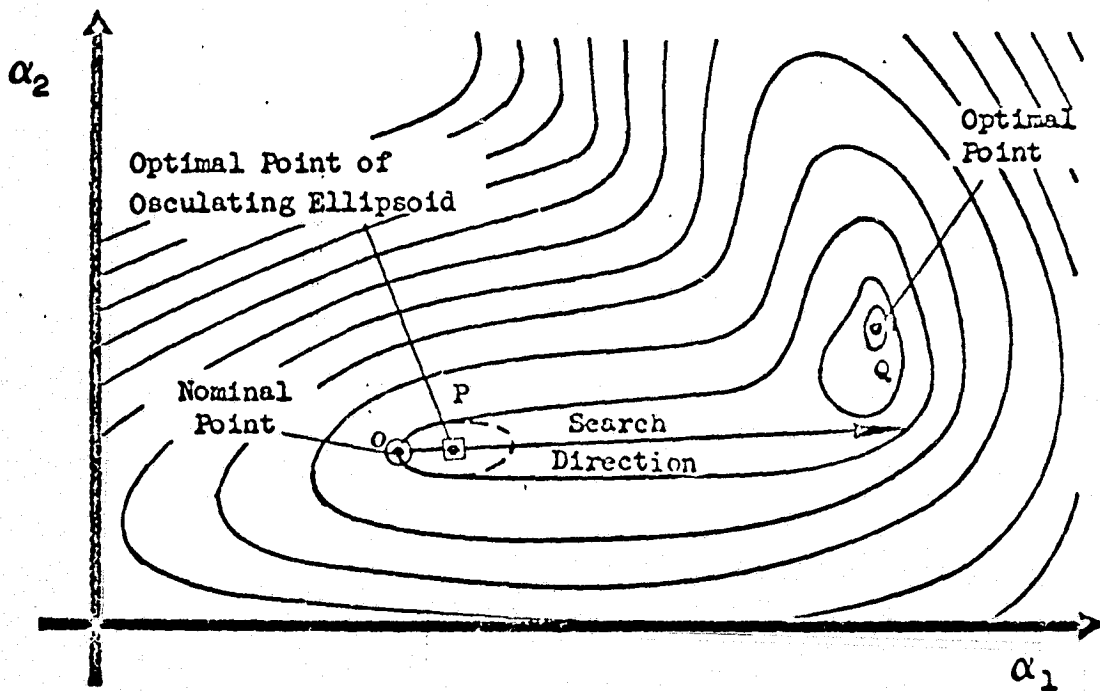**FIG. 12a.** - QUADRATIC SEARCH BEHAVIOR ON A NEAR
SECOND-ORDER SURFACE

FIG. 12b.- QUADRATIC SEARCH ON A HIGHER ORDER SURFACE

36

the manner described previously will lead to definition of the weighting matrix of equation (26), if the following formula is employed:

$$[W]_{i+1}^{-1} = [W]_i^{-1} + [A]_i + [B]_i \qquad (28)$$

where

$$[A]_i = \frac{\{\Delta\alpha\}_i \lfloor\Delta\alpha\rfloor_i}{\lfloor\Delta\alpha\rfloor_i \{\Delta \cdot \frac{\partial\phi}{\partial\alpha}\}_i} \qquad (29)$$

$$[B]_i = -\frac{[W]_i^{-1}\{\Delta \cdot \frac{\partial\phi}{\partial\alpha}\}_i \lfloor\Delta \cdot \frac{\partial\phi}{\partial\alpha}\rfloor_i [W]_i^{-1}}{\lfloor\Delta \cdot \frac{\partial\phi}{\partial\alpha}\rfloor_i [W]_i^{-1} \{\Delta \cdot \frac{\partial\phi}{\partial\alpha}\}_i} \qquad (30)$$

$$[W]_i^{-1} = [I] \qquad (31)$$

Here, $\lfloor\Delta\alpha\rfloor_i$ is the change in position during the ith one-dimensional search and

$$\lfloor \Delta \cdot \frac{\partial\phi}{\partial\alpha} \rfloor_i$$

is the change in gradient vector between the beginning and end of the ith one-dimensional search. On a numerically well-behaved function this technique may work well. It will find the optimum of an elliptic quadratic function in N successive searches. When appreciable numerical noise is present in the calculation, or when the one-dimensional extremal along the ray is not defined with precision, the method may produce erratic convergence, or convergence failure.

Pattern Search. In the present report, pattern search refers to a search which exploits a gross direction revealed by one of the other searches. The search algorithm is

$$\Delta\alpha_i = (\alpha_i^2 - \alpha_i^1) \cdot (DP), \qquad i = 1, 2, \ldots, N \qquad (32)$$

where α_i^2 and α_i^1 are the components of the control vector before and after the use of a preceding search technique. This type of search is illustrated in figure 13 following a section search. The combination of a section search and a pattern search in the problem illustrated leads directly to the neighborhood of the extremal. Repeated sectioning, on the other hand, would be a very slowly converging process due to the orientation of the contours with respect to the axes of the independent variables. It may be noted that a simple rotation of the independent variable axes by 45° results in sectioning alone becoming a rapidly converging process in this example. The pattern search can also be used to accelerate the steepest-descent process provided it follows two successive descents as in figure 14.

Adaptive Creeping Search. Adaptive creeping search is a form of small scale sectioning; however, instead of locating the position of the one-dimensional extremal on each section parallel to a coordinate axis, the coordiate is merely perturbed by a small amount, $\Delta\alpha_r$, in the descending direction.

The search commences with a small perturbation in one of the independent variables, α_r; a positive perturbation is first made; if this fails to produce a performance improvement, then a negative perturbation is tried. If neither of the perturbations produces an improved performance value, the variable retains its nominal value, and $\Delta\alpha_r$ is halved. If a favorable perturbation is found, the variable α_r is set to this value, and $\Delta\alpha_r$ is doubled. The process is repeated for each independent variable in turn, the order in which the variables are perturbed being *chosen randomly*. At this point an adaptive search cycle is complete, and the cycle is then repeated. A two-
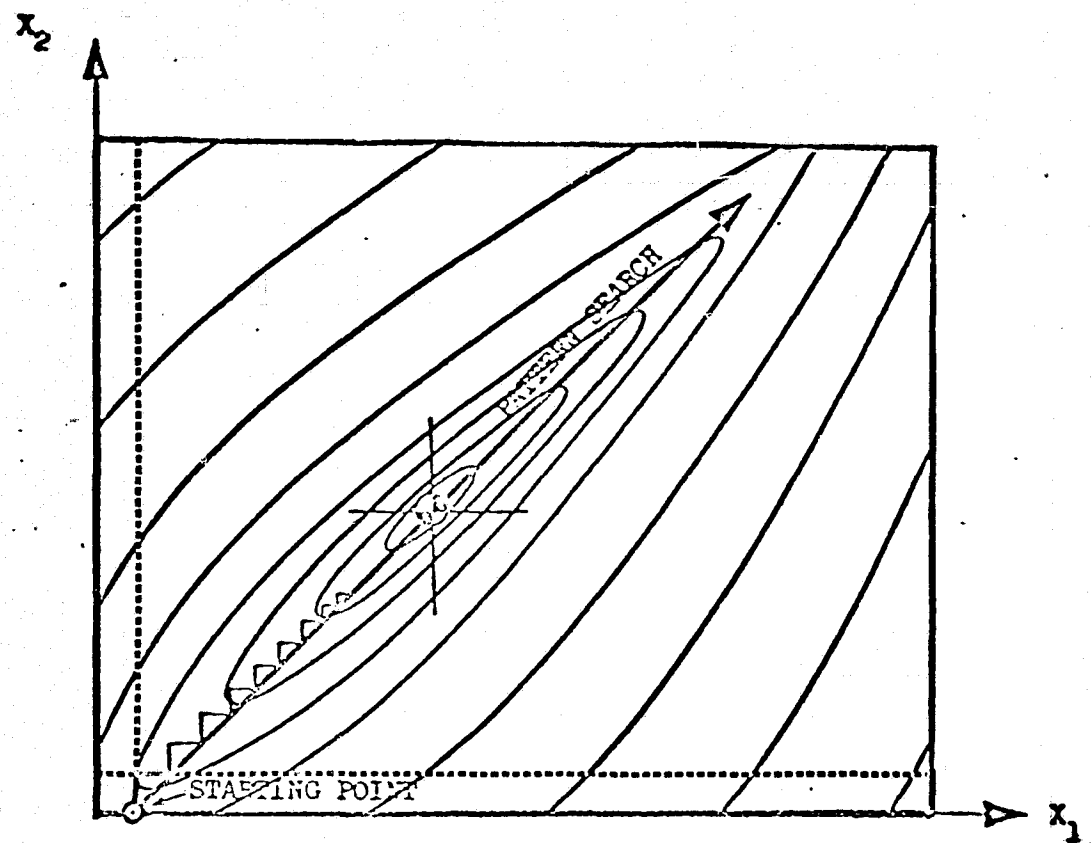
FIGURE 13. PATTERN SEARCH FOLLOWING SECTIONING
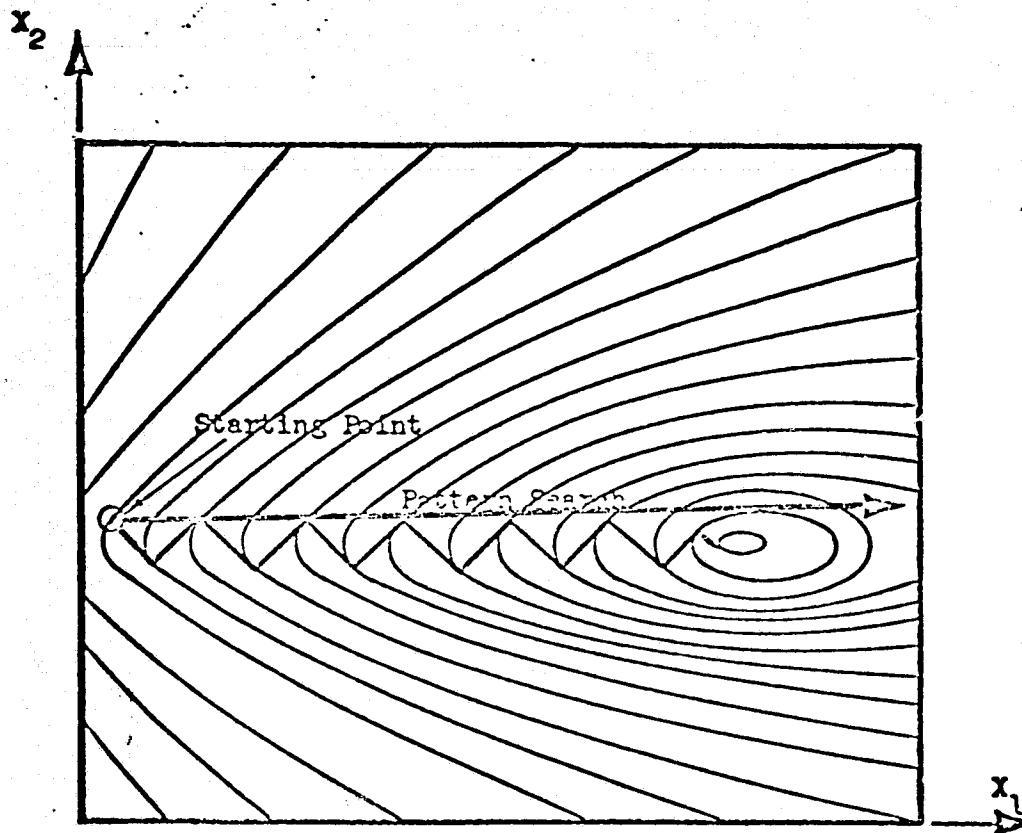
PARALLEL TO THE AXES

FIGURE 14.-PATTERN SEARCH FOLLOWING TWO STEEPEST-
DESCENT SEARCHES

dimensional illustration of this search is presented in figure 15. In the particular problem illustrated, the method converges rapidly reaching the neighborhood of the extremal within six evaluations.

The search algorithm can be written in the form

$$\Delta\alpha_r = 2.0^{(S_r - T_r)} \cdot (DP) \tag{33}$$

where S_r is the number of cycles in which the search has successfully perturbed the rth independent variable, and T_r is the number of cycles in which a perturbation of the rth variable has proved unsuccessful. While this search can be looked upon as a one-dimensional approach, this viewpoint is somewhat artificial. Here, the scalar quantity (DP) merely defines an initial perturbation for each independent variable. Once started the search proceeds inevitably to its conclusion, the perturbation in each independent variable being adaptively determined according to equation (33) on the basis of the performance function response contour behavior encountered during the particular problem solution. This search can be quite efficient when used in combination with the pattern search acceleration procedure.

Magnification. When studying discrete models of continuous systems of the type encountered in certain engineering problems such as aerodynamic shaping or structural design problems, there is a tendency on the part of some search algorithms to achieve a favorable shape before satisfying the desired constraint levels. In such cases, when it is known that the unconstrained extremal is the null vector, a simple magnification search can lead to rapid convergence to the desired solution. The magnification algorithm is

$$\Delta\alpha_i = \alpha_i \cdot (DP), \qquad i = 1, 2, \ldots, N \tag{34}$$
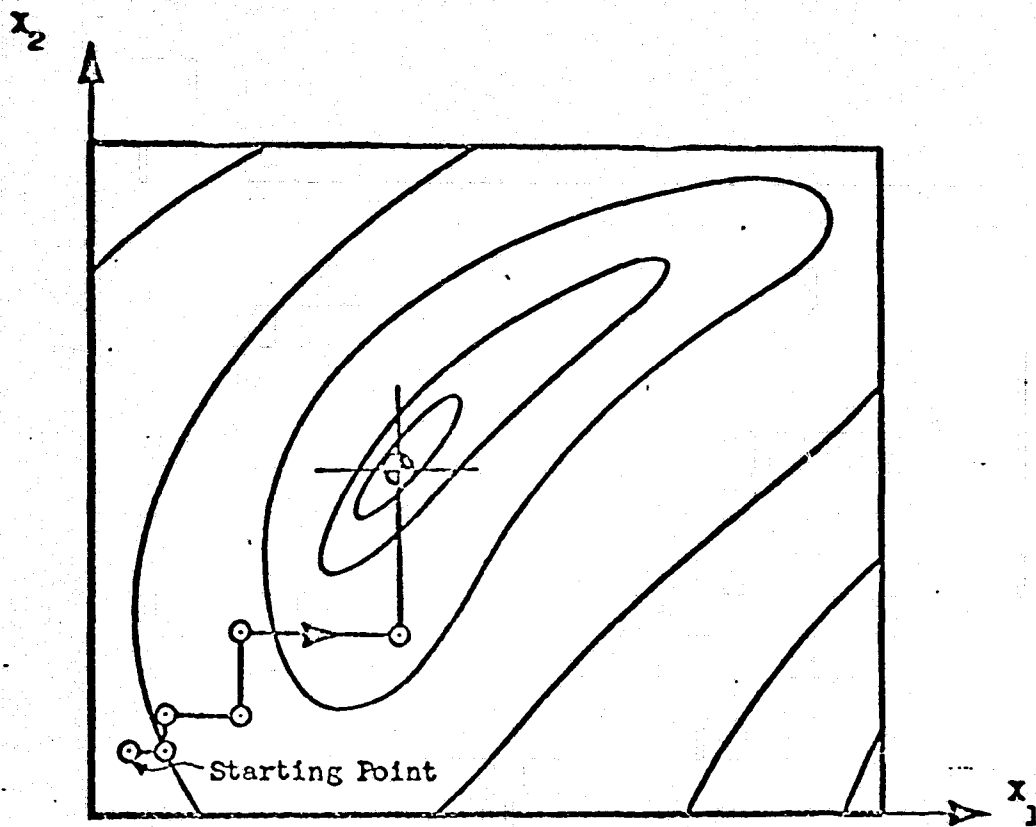
41

FIGURE 15. —ADAPTIVE SEARCH

Here (DP) is positive and all components of the control vector are to be simultaneously perturbed. Generally, the unconstrained extremal point corresponds to the null vector; this method may prove efficient.

Arbitrary Ray Search. In practical design optimization a search along an arbitrary multidimensional ray can be of utility. For example, when two *minimal extremal* solutions appear to be possible, a search on the ray connecting the two points should reveal the presence of a *maximal extremal* somewhere on the ray between the two minimal extremals. The algorithm for this search is

$$\Delta\alpha_i = (\alpha_i^2 - \alpha_i^1) \ (DP), \quad i = 1, 2, \ldots, N \qquad (35)$$

where α_i^1 and α_i^2 are the two minimal extremal points. In general, α_i^1 and α_i^2 may be any two points in the control space.

Random Point Search. A straightforward Monte-Carlo search which examines point designs distributed in a uniform random manner within the feasible region is often of utility when the response surface is of a complex nature. Such a search is included in the AESOP code primarily for use as a nominal point design generation procedure.

AIRFOIL OPTIMIZATION RESULTS

Results have been obtained for a number of different low
speed (M = .1) aerodynamic shaping problems of practical
interest. Potential flow analysis is based on solution of the
two-dimensional potential flow equation

$$(a^2 - u^2) \, \phi_{xx} + (a^2 - v^2) \, \phi_{yy} - 2uv \, \phi_{xy} = 0$$

where ϕ is the velocity potential, u and v are the velocity
components

$$u = \phi_x, \quad v = \phi_y$$

and a is the local speed of sound determined from the energy
equation and the stagnation speed of sound

$$a^2 = a_o^2 - (\frac{\gamma - 1}{2}) \, (u^2 + v^2)$$

Solutions are obtained by Jameson's finite difference scheme,
reference 10.

The study used all of the numerical search methods described
above. The nominal airfoil configuration was the NACA 64-206
airfoil. This airfoil was subject to modifications which en-
hance its aerodynamic capabilities. The modification was the
sum of two components:

a. A continuous binomial additional thickness distribution,
   applied to the upper surface, of the form,

$$\delta y_t(x) = A \, x^{\varepsilon_1} (1 - x)^{\varepsilon_2} \qquad (0 \leq x \leq 1)$$

where A, ε_1, and ε_2 are variable parameters to be
optimized by multivariable search. The quantity A
is given by

$$A = \frac{\bar{y}(\varepsilon_1 + \varepsilon_2)^{\varepsilon_1 + \varepsilon_2}}{\varepsilon_1^{\varepsilon_1} \varepsilon_2^{\varepsilon_2}}$$

where $\bar{y}$ is the maximum additional thickness to the airfoil.

b. An additional camber distribution of the form,

$$\delta y_c(x) = \begin{cases} y_c[1 - \left(\frac{x_c - x}{x_c}\right)^{\epsilon_3}] & (0 \leq x \leq x_c) \\ y_c[1 - \left(\frac{x - x_c}{1 - x_c}\right)^{\epsilon_4}] & (x_c \leq x \leq 1) \end{cases}$$

where x_c, y_c, ϵ_3, and ϵ_4 are variable parameters to be selected by multivariable search. These parameters denote the location and geometric form of the camber of both upper and lower surfaces.

The seven independent parameters of these equations can be used to generate a variety of curves, many of which, however, are impractical for airfoils. Nevertheless, it is important to note that the thickness and camber distributions are both "smooth", so that the slope is continuous everywhere except at the leading and trailing edges of the airfoil. Also, it will be found that certain of the parameters can be varied only through rather small numerical ranges, in order to retain important practical features of the airfoil.

Results are presented below in three sections, corresponding to the following specific applications:

1. Unconstrained optimization of high-camber airfoil,

2. Comparative search optimization of low-camber airfoil, and

3. Constrained optimization of low-camber airfoil.

The principal purpose of the present study is a demonstration of the versatility and relative efficiency of various multivariable search options of the AESOP code in the two-dimensional airfoil shaping problem. The applications can

therefore be regarded as representative, rather than exhaustive. This also means that the results obtained can be easily extended to include other optimization criteria or other values of the reference airfoil or shaping parameters.

High-Camber Unconstrained Airfoil Optimization

To demonstrate the AESOP code in the optimization of the general airfoil shaping problem, a seven-parameter modification to the NACA 64-206 airfoil was tested. The performance criterion was the lift coefficient of the airfoil, and all of the shaping parameters were allowed to vary for this purpose.

Each of the parameters was given an initial value and extreme upper and lower values, as listed in Table I below.

	Parameter	Minimum	Initial	Maximum
Thickness (upper)	$\bar{y}$	0	.06	.09*
	ϵ_1	.25	1.0	1.0*
	ϵ_2	1.0*	1.0	3.0
Camber (upper & lower)	x_c	.1	.25	.9*
	y_c	0	.005	.04*
	ϵ_3	1.0	2.0	3.0*
	ϵ_4	1.0	2.0	3.0*

TABLE I. INPUT PARAMETER VALUES IN LIFT MAXIMIZATION
(*Signifies optimal parameter value.)

The optimization procedure was limited to 50 iterations using uniform random ray and pattern searches. No other constraints were placed on the aerodynamic or geometric properties of the airfoil.

46

The results of the optimization study can be presented both graphically and numerically. The final, optimal airfoil and its associated pressure distribution are shown in Figure 16, and the terminal values of the parameters are all at their maximum values, except for ϵ_2, which is at its minimum allowable value (see Table I).

The following observations can be made concerning these results:

1. The thickness and camber parameters have been combined to give a configuration resembling a flapped airfoil, which is a standard method of increasing the lift coefficient.

2. The shape of the airfoil is such that separation would occur near the trailing edge of the upper surface if leading edge stall did not occur first. The pressure and lift coefficients are therefore somewhat unrealistic, and would presumably require refinement using a viscous theory.

3. The methods of optimization used are the random ray and pattern search methods, and no improvements in lift were obtained after the 19th iteration, for all parameters are then at their bounding values. The initial lift coefficient of 1.347 is increased to 2.770, as shown in Figure 17(a). This is the limiting theoretical lift coefficient for the parameter range studied.

4. The adverse pitching moment increases with the lift. As shown in Figure 17(b), this variation is nearly linear, as was found in earlier optimization studies (References 7 through 9).

For this example, it is seen that practically all performance improvements occur between iterations 11 and 18. This type of response will be characteristic of unconstrained optimization
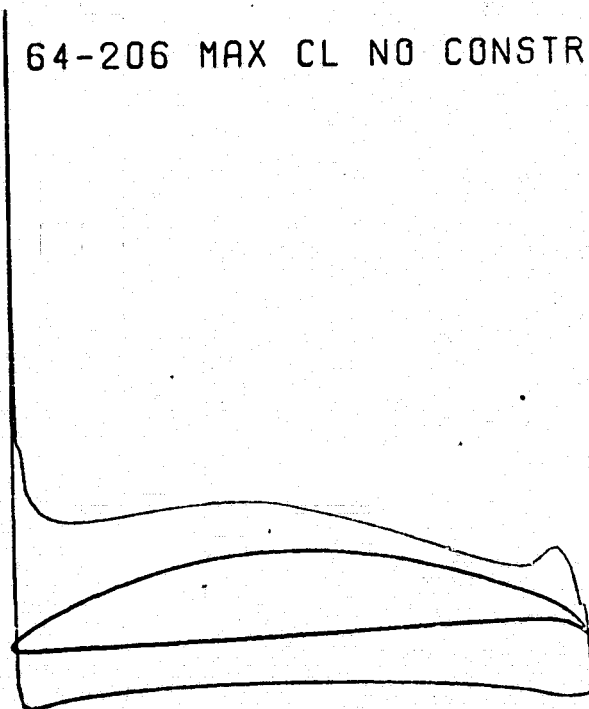
64-206 MAX CL NO CONSTRAINTS

FIGURE 16.   MAXIMUM LIFT, NO CONSTRAINTS ON C_M OR $C_{P_{MAX}}$

All parameters achieve limiting
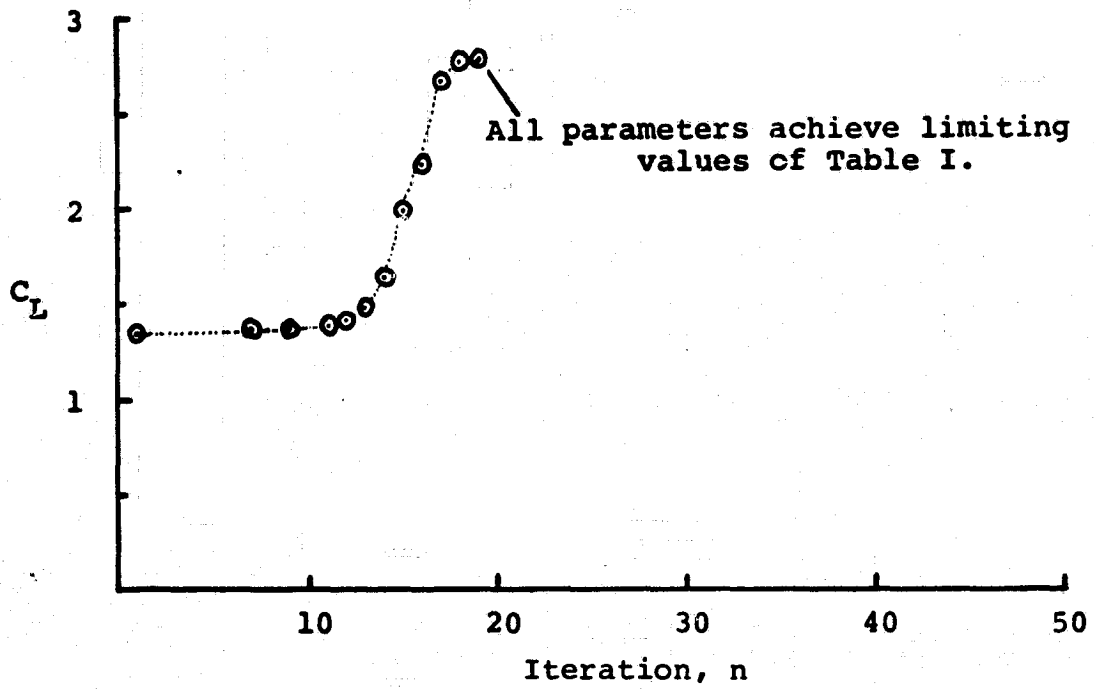values cf Table I.

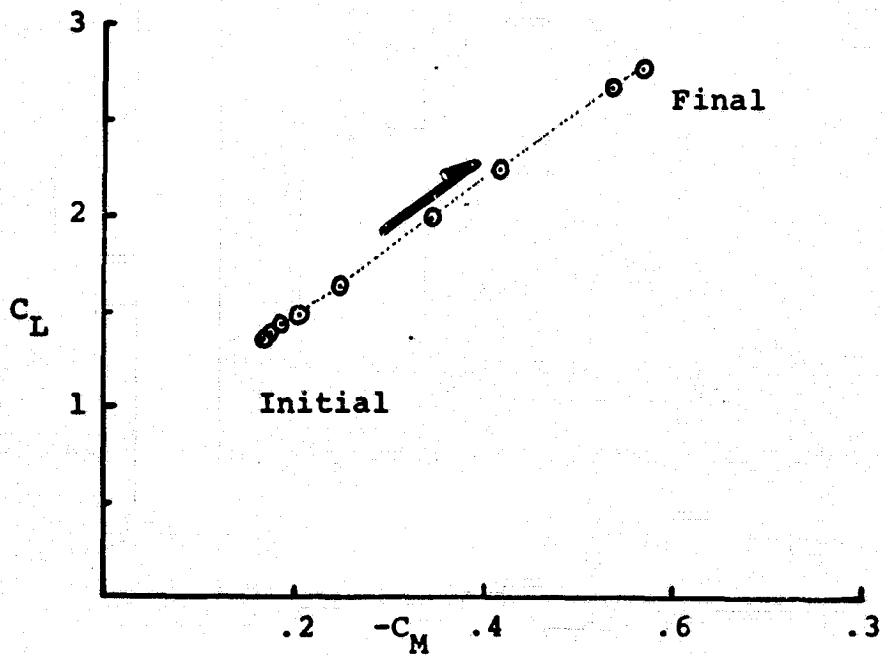FIGURE 17(a). LIFT MAXIMIZATION, NO CONSTRAINTS

FIGURE 17(b). PITCHING MOMENT CORRESPONDING TO LIFT MAXIMIZATION

problems which are solved using effective numerical methods. Another conclusion of this study is that the constraints can comprise an important part of the input data. Thus, in this example, the peak pressure coefficient changed from -5.84 to -11.01, but if it had been constrained to a more realistic level (greater than -4.0) a very different airfoil contour would have resulted.

Low-Camber Comparative Search

This portion of the study served to compare the different methods of optimizing airfoil performance. For brevity the comparison was done with the emphasis on the upper-surface parameters, $\bar{y}$, ϵ_1 and ϵ_2. Two nominal configurations were examined, corresponding to approximately 3% and 6% additional thickness variations. The nominal values of the seven parameters, and the corresponding calculated aerodynamic characteristics of the resulting airfoil at $M = .1$ and $\alpha = 6^{\circ}$, are given in Table II. The geometric appearance of the airfoil, and the pressure distribution about the airfoil are shown for the 6% modification in Figure 18 using the parameter values $\bar{y} = .06$, $\epsilon_1 = \epsilon_2 = 1.0$.

The following representative optimization criteria were chosen for the present brief study:

a. Minimize peak pressure $\left| C_{P_{max}} \right|$

b. Maximize lift (C_L)

c. Maximize lift (C_L) for a given moment (C_M)

Additional input data relates to the optimization methods to be used, the number of iterations to be computed, and the tolerances permitted on any constraints.
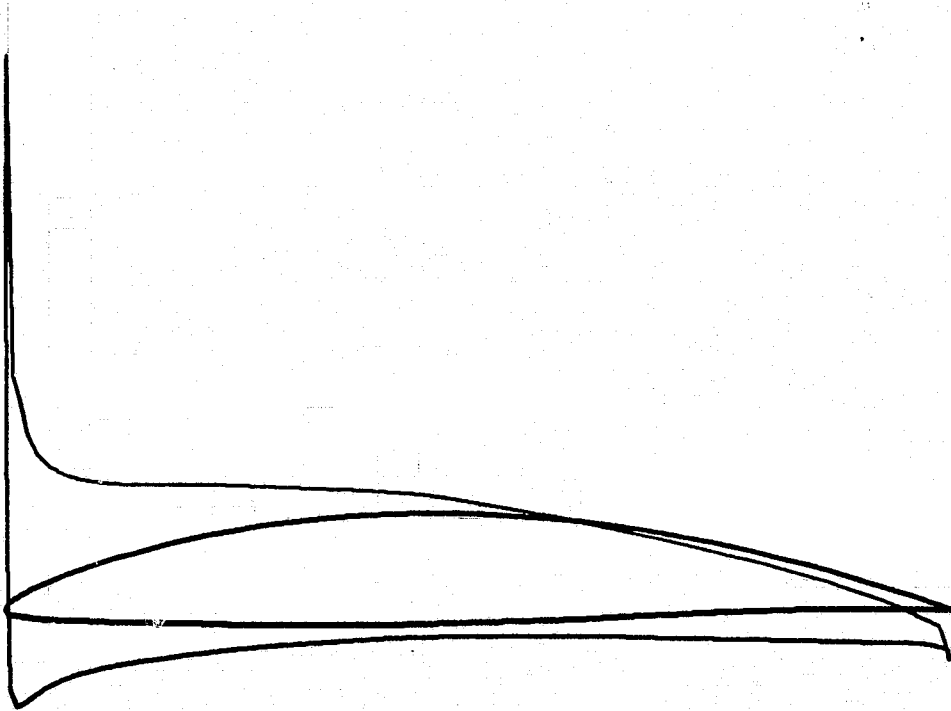
FIGURE 18.   NOMINAL MODIFIED 64-206 AIRFOIL, $\bar{y} = .06$, $\varepsilon_1 = 1$, and $\varepsilon_2 = 1$

Parameter	Mod. 1	Mod. 2
$\bar{y}$	.06	.03
ϵ_1	1.0	.75
ϵ_2	1.0	1.0
x_c	.25	.25
y_c	.005	.005
ϵ_3	2.0	1.75
ϵ_4	2.0	2.0
C_L	1.347	1.086
C_m	-.168	-.094
$-C_{p_{max}}$	-5.844	-5.191

TABLE II.   NOMINAL AIRFOIL CHARACTERISTICS

a. Minimize Peak Pressure

Minimization of the high pressure peak at the leading edge of the reference airfoil at M = .1 and α = 6°, is a good illustrative performance criterion, because small geometric airfoil changes can cause large variations in this pressure value. Results were obtained using 11 different optimization methods, all of which cycled through 100 iterations on airfoil modification 1 of Table II. The results of these calculations are presented in Figure 19, which show the improvements in peak pressure as a function of iteration number. Also shown in these Figures are the

final airfoil shape and pressure distributions. It is seen that several methods converge quickly to the minimum "optimal" value, while other methods perform poorly. The eleven methods are ranked in order of final pressure coefficient in Table III, which sums up the final values of Figure 19. Notice that the best results follow from randomized and one parameter at a time search methods, while "steepest descent" and "quadratic" methods give very poor results. It should be noted that the computational times include compiling several subroutines, program reassembly, loading the combined Jameson/ASEOP codes and computer generated plotting. Computation times would be smaller if an absolute program element were employed, plots omitted and only the relevent parts of AESOP employed. Nevertheless, the computational times quoted serve to measure the relative effectiveness of the eleven searches.

Method	$\left\|c_{p_{max}}\right\|$	Iterations	Comp. Units for 100 Iterations
Uniform Random Ray	1.68	32	1105
Creeper	1.73	64	1029
*Davidon	1.77	98	1083
Directed Random Ray	1.85	24	1156
Sectioning (12 Evaluations on ID Search)	1.86	52	1351
*Steepest Descent (Variable W)	1.96	81	1112
Sectioning (6 Evaluations on ID Search)	2.00	42	966
Monte Carlo	2.10	13	290***
*Jacobson (Homogeneous Functions)	4.09	87	682
*Steepest Descent (W = I)	5.40	98	875
**Quadratic	5.74	59	728

* Methods using 1st derivatives

** Method using 1st and 2nd derivatives

*** Only ran 15 airfoils

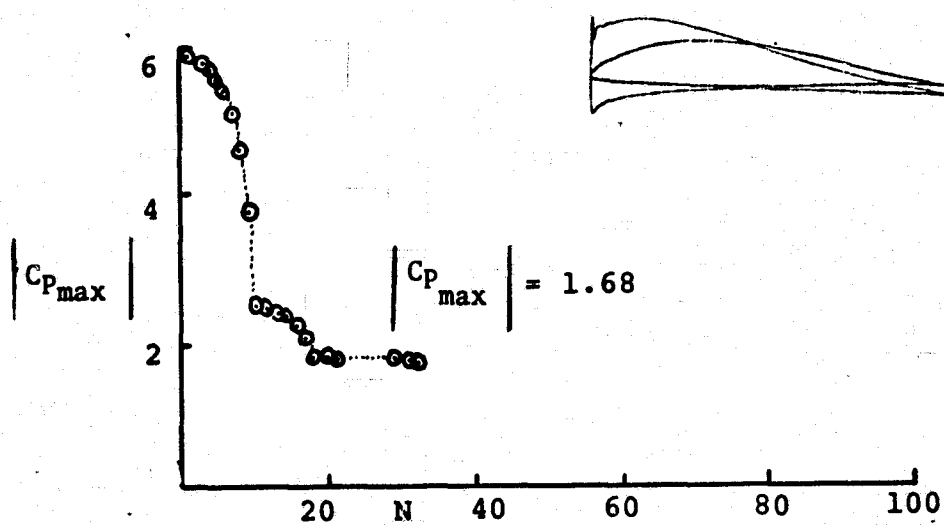TABLE III. RELATIVE PERFORMANCE OF OPTIMIZATION METHODS.

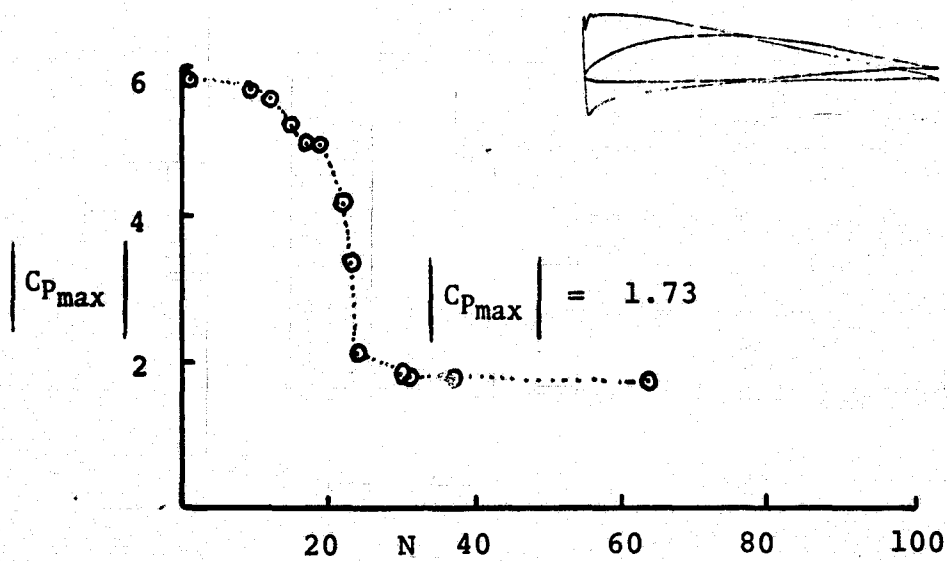FIGURE 19(a).   UNIFORM RANDOM RAY METHOD
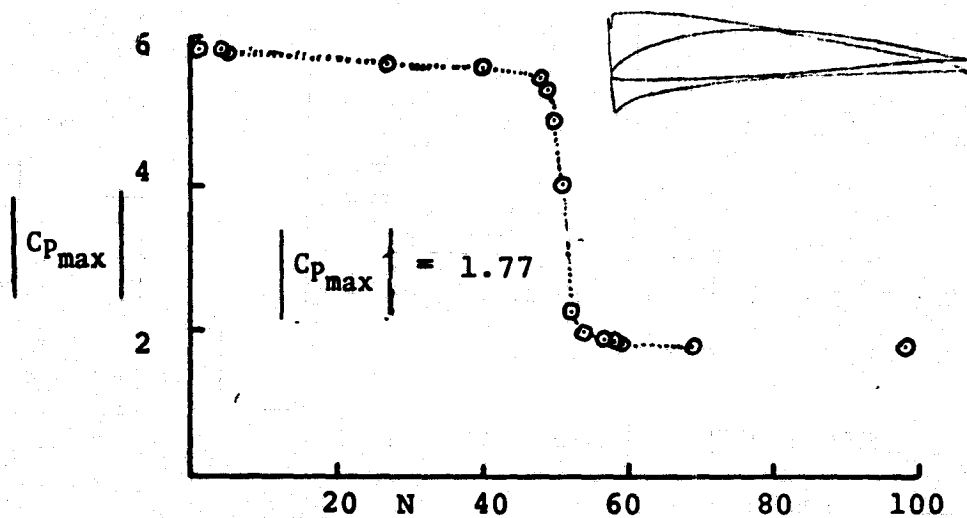

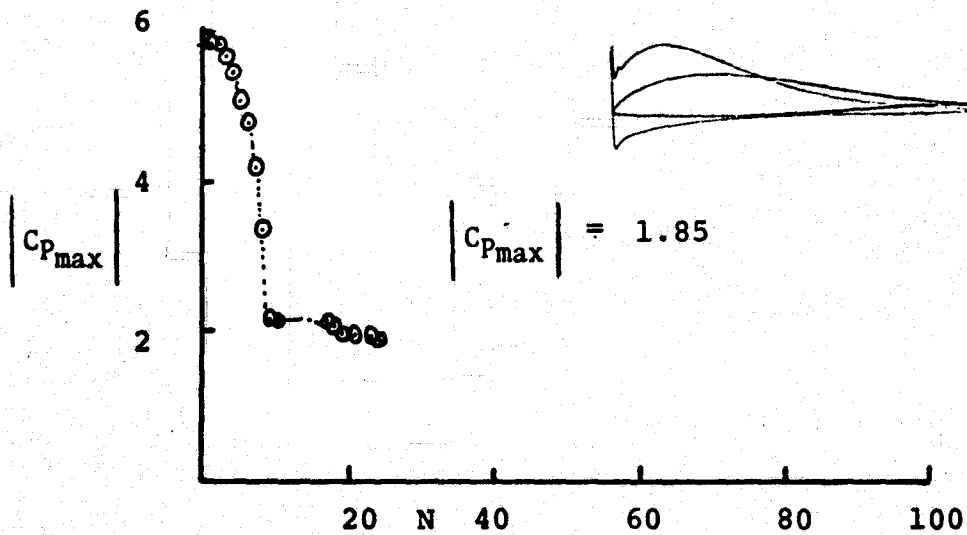FIGURE 19(b).   CREEPER METHOD

FIGURE 19(c).   DAVIDON METHOD
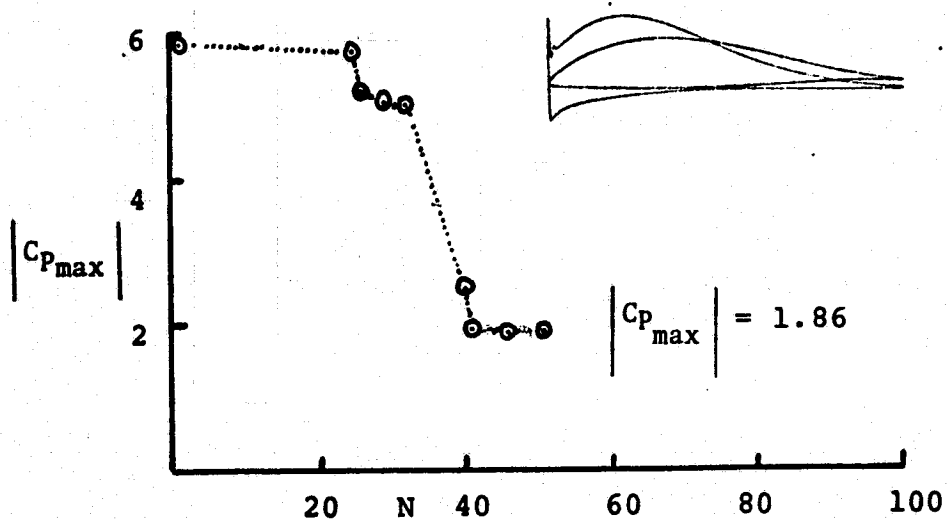

FIGURE 19(d).   DIRECTED RANDOM RAY METHOD
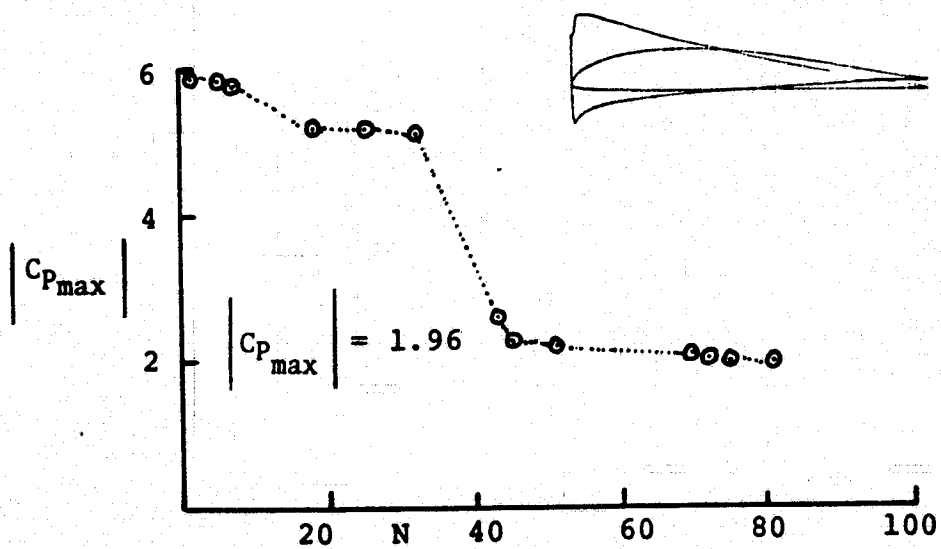
55

FIGURE 19(e).   SECTIONING METHOD

$\left| C_{P_{max}} \right| = 1.86$

FIGURE 19(f).   STEEPEST-DESCENT METHOD (VARIABLE W)
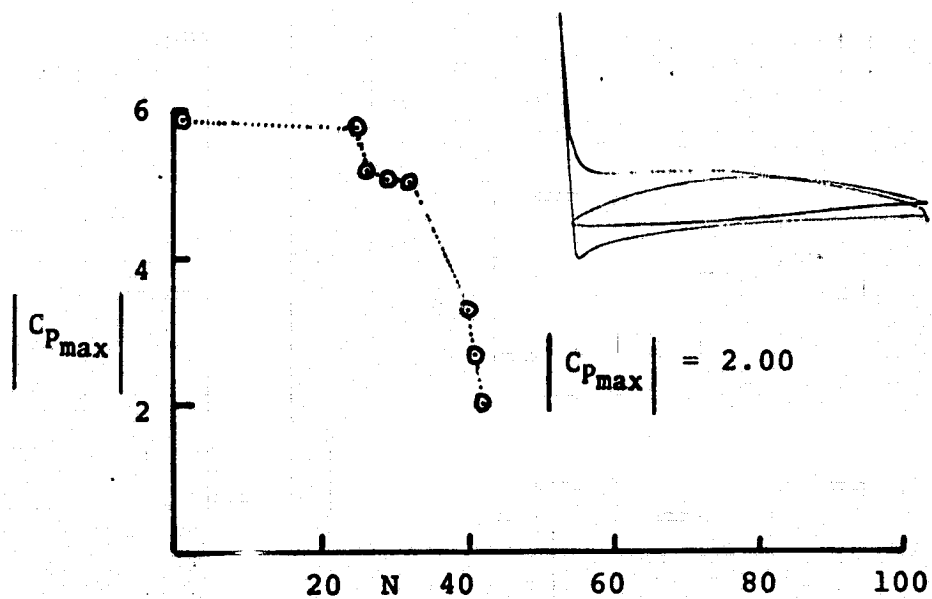
$\left| C_{P_{max}} \right| = 1.96$

FIGURE 19(g). SECTIONING METHOD
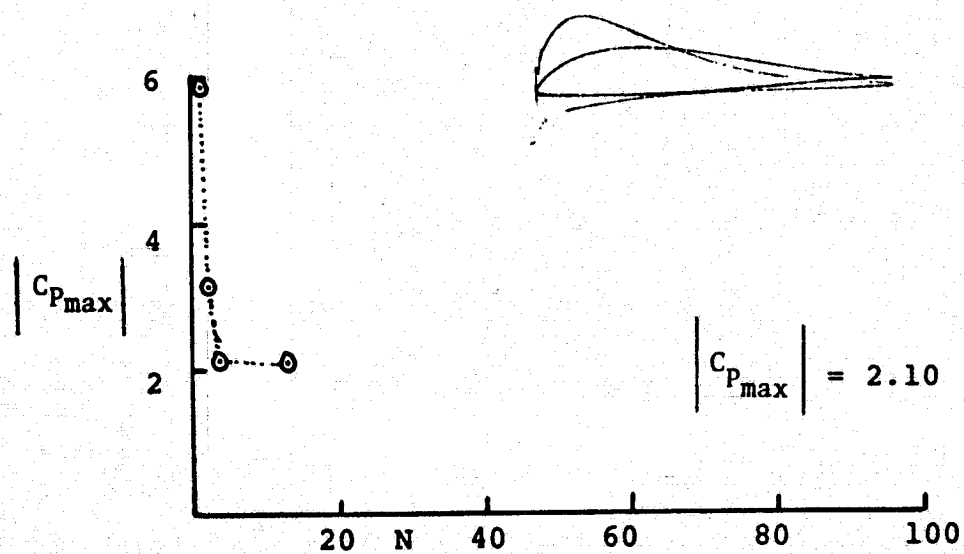

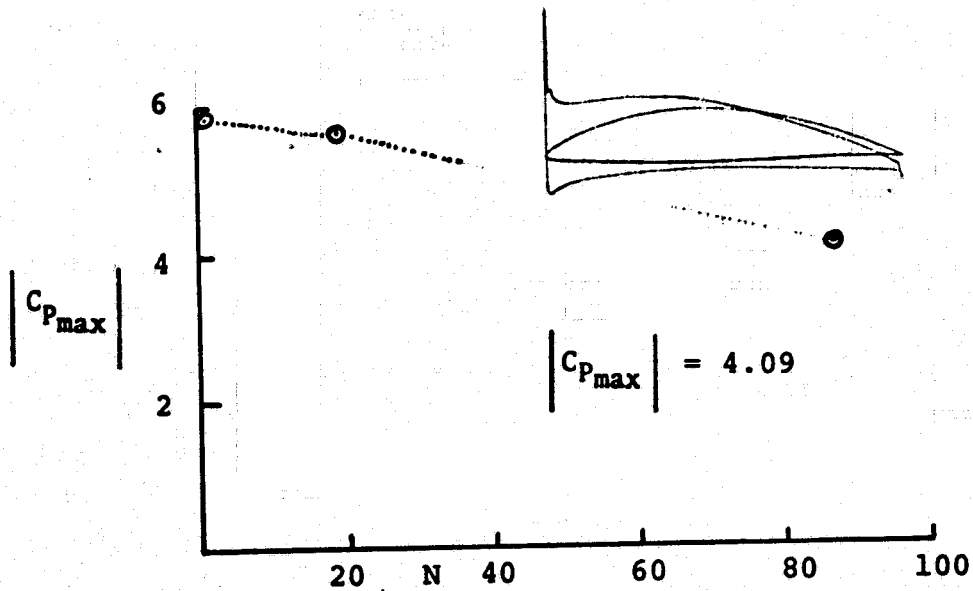FIGURE 19(h). MONTE CARLO METHOD
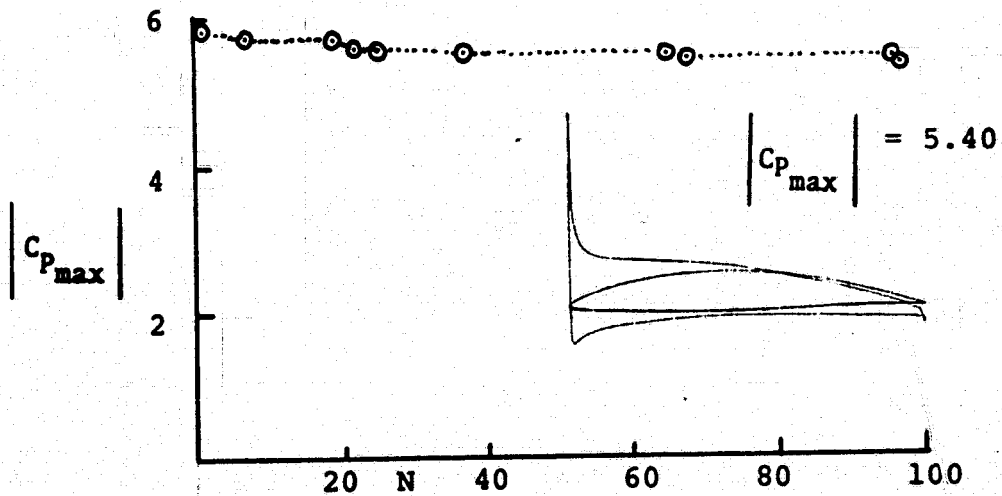
57

FIGURE 19(i). JACOBSON METHOD

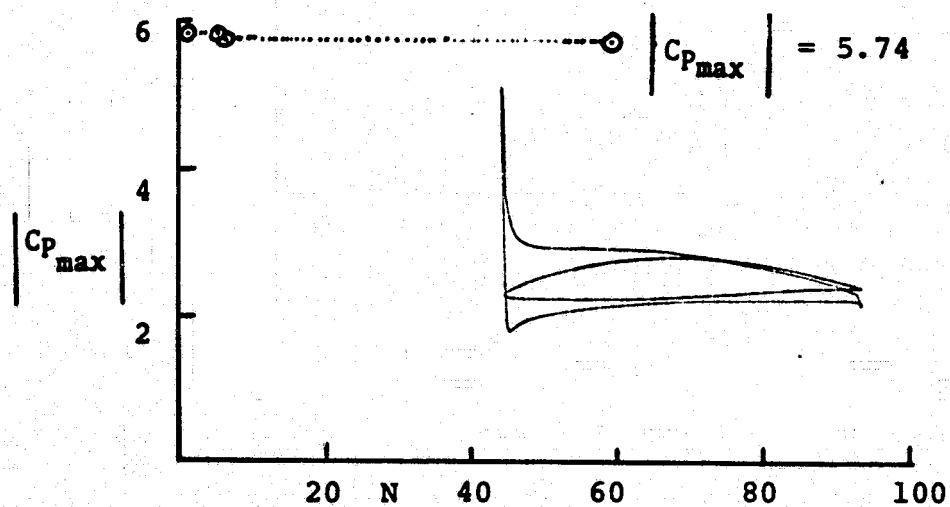FIGURE 19(j). STEEPEST-DESCENT METHOD (W = I)

58

FIGURE 19(k).   QUADRATIC METHOD

The large variations in these "optimal" airfoil shapes emphasize that certain numerical methods are much better than others in this type of application, and that speed of convergence should be a major consideration in the choice of numerical algorithm. The ranking of the results is roughly in the same order as the computational cost, as measured in the last column of Table III. Computation times can be significantly reduced by elimination of the coding associated with searches not used in a given calculation. This was not done in the present study however. It can also be noted (Reference 9) that the five best methods developed airfoils which have two equal pressure peaks on the upper surface, but which are otherwise noticeably different. In cases where two peaks are developed the forward sharp pressure peak tends to be a result of the potential flow analysis employed. In real flows this forward peak is modified by viscous effects. Once an airfoil having two equal pressure peaks is developed by the searches further progress in the Cp minimization becomes more difficult for only those airfoil perturbations which simultaneously reduce both peaks provide further improvement.

b. Maximize Lift

The lift coefficient was again chosen as a performance criterion for airfoil modification 2, and four optimization methods were compared in a 50 iteration test. The thickness parameter $\bar{y}$ was allowed to vary over the interval $0 \le \bar{y} \le .06$, and the exponents for the leading and trailing edges were required to satisfy $.25 \le \epsilon_1 \le 1.0$, and $1.0 \le \epsilon_2 \le 3.0$, respectively. The absence of camber parameters excludes the possibility of developing a "flap-like" airfoil having a very high lift coefficient.

The results of the optimization methods are shown in Figure 20, and it is seen that the methods produce essentially equal lift coefficients. All of the methods (directed random ray, uniform random ray, steepest descent, and creeper) converged to the maximum additional thickness after 20 to 30 iterations, after which no further gains in lift were generated for limiting
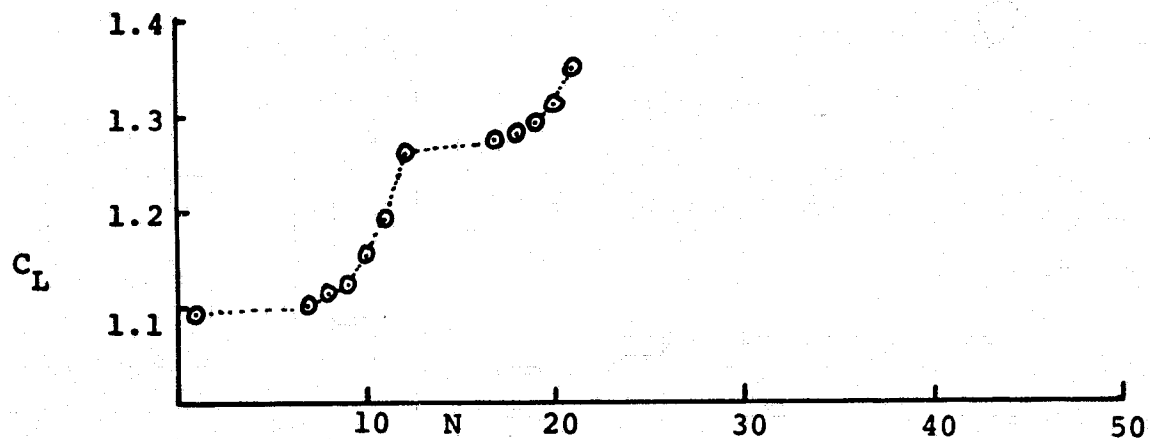
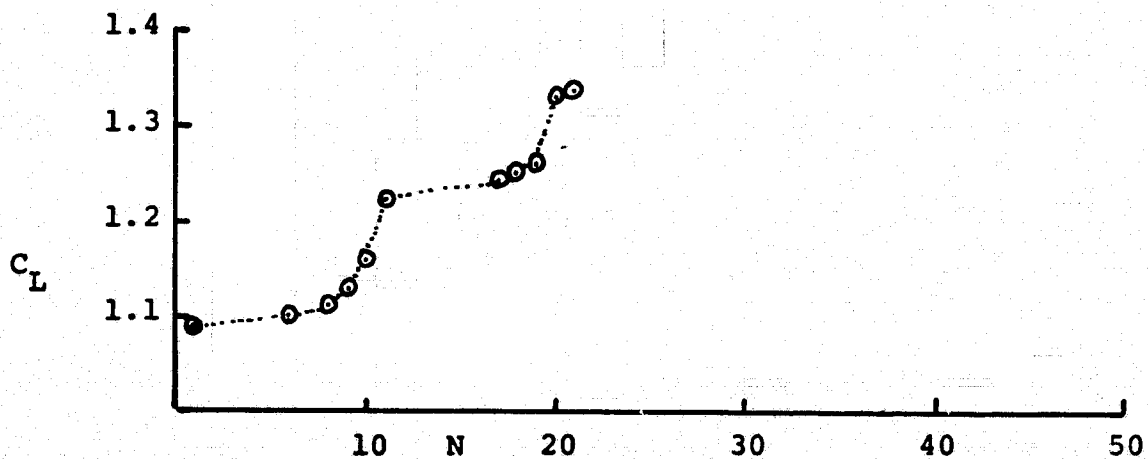FIGURE 20(a).   DIRECTED RANDOM RAY METHOD
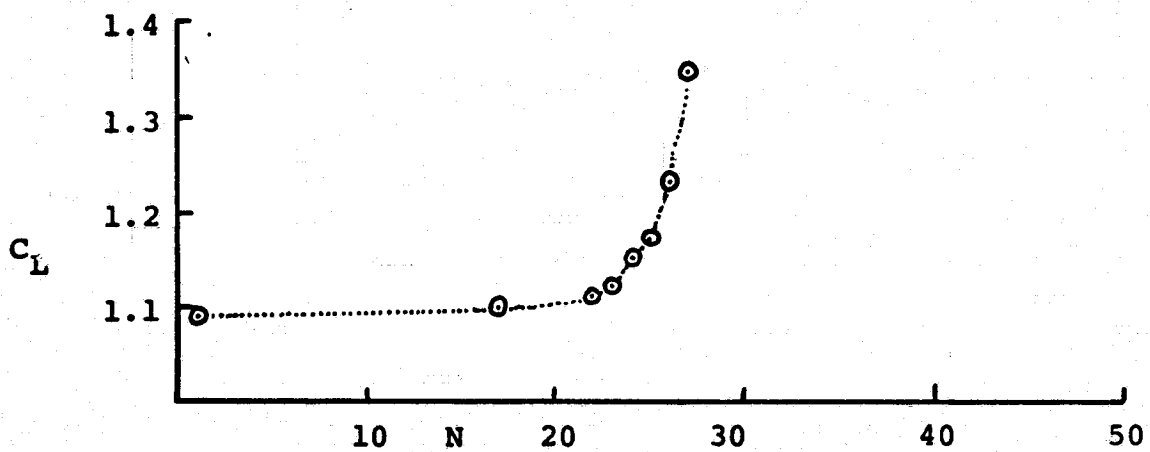

FIGURE 20(b).   UNIFROM RANDOM RAY METHOD

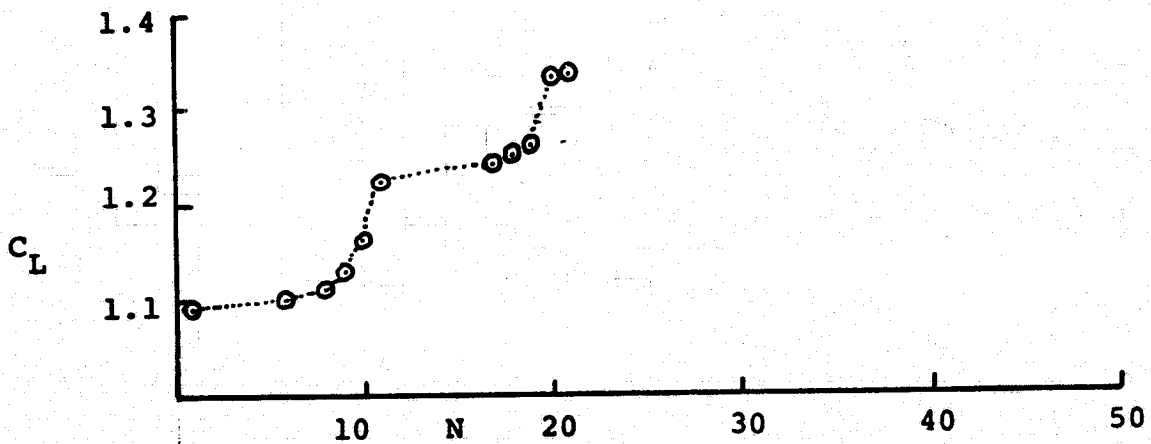FIGURE 20(c). CREEPER METHOD

FIGURE 20(d). STEEPEST-DESCENT METHOD

62

values of the exponents were attained. These values were $\bar{y}$ = .06, ϵ_1 = ϵ_2 = 1.0. The final values of lift, moment and pressure coefficients are as given in Table IV.

Method	C_L	C_m	$C_{p_{max}}$
Directed Random Ray	1.347	-.168	5.842
Uniform Random Ray	1.342	-.165	5.572
Steepest Descent	1.347	-.168	5.843
Creeper	1.347	-.168	5.843

TABLE IV. LIFT MAXIMIZATION BY FOUR NUMERICAL METHODS

c. Maximize Lift for a Given Moment

The incorporation of a constraint function into the optimization problem adds realism to the problem statement. In the present case, the desired moment coefficient was chosen at a moderate   but representative value, C_M = -.1, and airfoil modification 1 was taken as the nominal airfoil. The significant initial airfoil parameters and associated lift, moment and pressure coefficients have been given in Table II.

The additional thickness parameters were then adjusted using a combination of pattern and random ray techniques, with results as summarized in Figure 21. The actual computation was carried out for the unconstrained maximization of the performance index,

$$J = C_L - k (C_M - .1)^2$$

so that the degree of violation of the constraint can be controlled by the choice of the scalar, k. In the present case, it was given the initial value 10,000. This constraint

penalty weighting function value is then internally adjusted in the AESOP code.

The final values of the significant parameters were:

$$\bar{y} = .0867$$

$$\varepsilon_1 = .895$$

$$\varepsilon_2 = 1.678$$

all of which are in the mid-range of the allowable values of the parameters. As shown in Figure 21, the moment constraint initially causes the lift to decrease, after which a modest steady increase in lift is achieved. The initial airfoil shape and pressure distributions have been shown in Figure 18, and the final results are given in Figure 22, which shows the strong sensitivity of the pressure distribution to small changes in the parameters. The final values of the lift, moment and peak pressure coefficients in this example are:

$$C_L = 1.255$$

$$C_M = -.105$$

$$\left| C_{P_{max}} \right| = -1.860$$

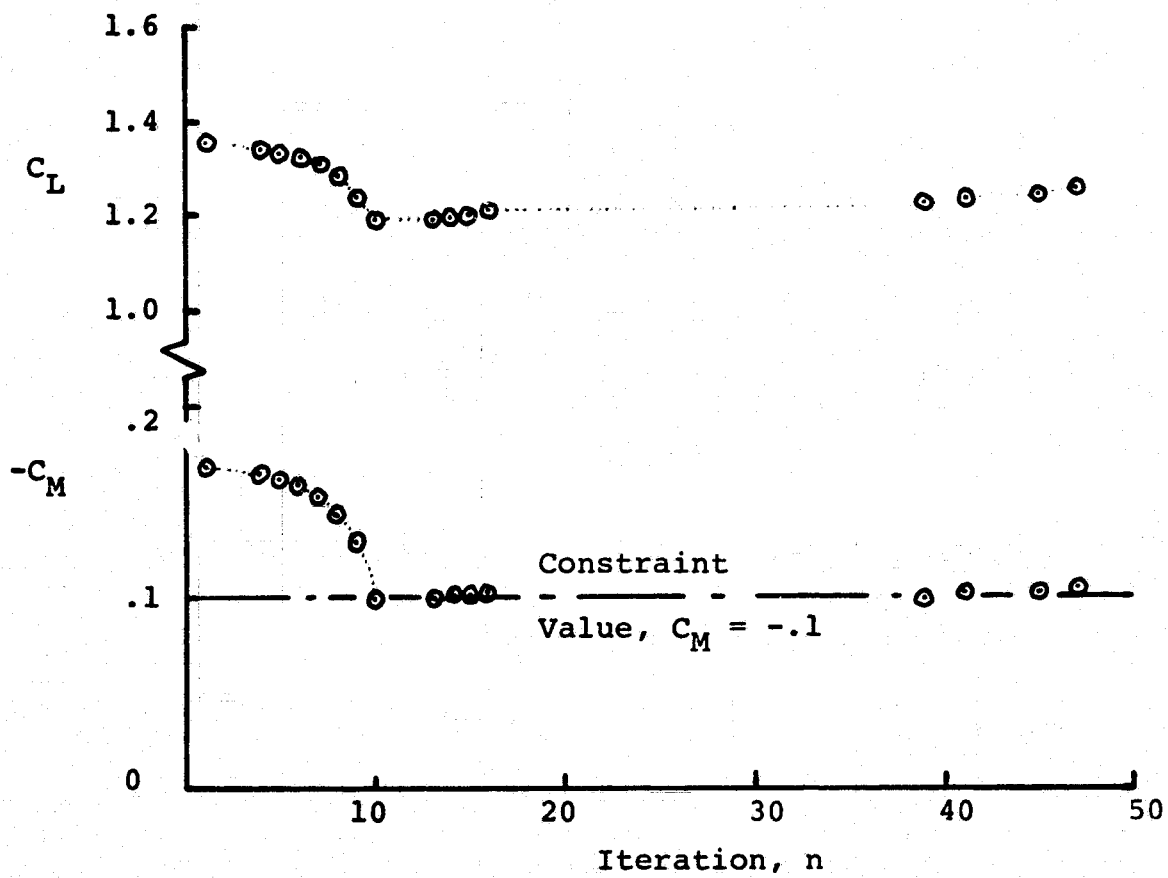and here again as in some previous solutions it is noted that the two upper surface pressure peaks are equal.

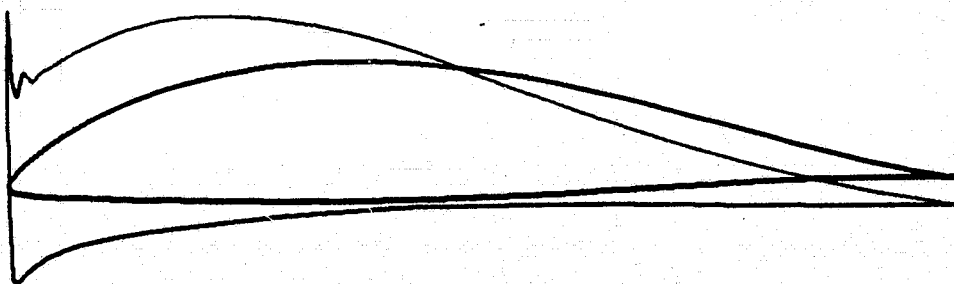FIGURE 21. LIFT MAXIMIZATION WITH CONSTRAINED MOMENT

FIGURE 22.   64-206 MAXIMIZE LIFT COEFFICIENT
WITH CM = -.1

CONCLUSION

The ability of multivariable search procedures in the solution of two-dimensional non-linear inviscid low speed aerodynamic shaping problems has been examined. In general the non-linear inviscid optimization problem yields results as readily as the linear inviscid problem, Reference 11. Elementary one parameter at a time and random techniques appear to achieve better results than organized searches which require derivatives. Only one organized search out of those employed comes near to the elementary searches in solution of the present problems. This organized search is the first-order Davidon method.

It is clear from these results that <u>unconstrained lift maximization</u> is primarily accomplished by modifications to the airfoil trailing edge. In particular this is accomplished by the generation of "flap-like" airfoils.

When <u>pressure peak magnitude is reduced</u> the more successful searches define an airfoil which has two equal pressure peaks. The first peak lies near the leading edge. The second peak is 30% to 40% aft of the leading edge and is of a broader more gradual nature than that at the leading edge. The forward peak is both sharper and narrower, and would be considerably attenuated by the effects of viscosity. Subject to the limitations of the viscous theory, however, the pressure optimization process yields a logical conclusion.

It is clear that significant modifications can be made to an existing airfoil using a few carefully selected shaping parameters. At low speeds three parameters appear to be sufficient for upper surface shaping, seven parameters suffice for both upper and lower surface shaping. Use of a small number of shaping parameters for two dimensional airfoil shaping indicates that successful three dimensional shaping is quite feasible at the present time.

REFERENCES

1. Hague, D.S. and Glatt, C.R. An Introduction to Multi-variable Search Techniques for Parameter Optimization. NASA CR-73200. 1968.

2. Hague, D.S. and Glatt, C.R. A Guide to the Automated Engineering and Scientific Optimization Program, AESOP. NASA CR-73201. April 1968.

3. Hague, D.S. and Glatt, C.R. Application of Multivariable Search Techniques to the Optimal Design of a Hypersonic Cruise Vehicle. NASA CR-73202. 1968.

4. Wilde, D.J. Optimal Seeking Methods. Prentice-Hall. 1964.

5. Hague, D.S. Three-Degree of Freedom Problem Optimization Formulation, Part I, Vol. 3. FDL-TDR-64-1. 1964.

6. Hague, D.S. "The Optimization of Multiple-ARC Trajectories by the Steepest-Descent Method," Recent Advances in Optimization Techniques, John Wiley, 1966, pp. 489-517.

7. Merz, A.W. and Hague, D.S. An Investigation on the Effect of Second-Order Additional Thickness Distributions to the Upper Surface of an NACA 64-206 Airfoil. Aerophysics Research Corporation TN-195. February 1975.

8. Hague, D.S. and Merz, A.W. Theoretical Effect of Modification to the Upper Surface of Two NACA Airfoils using Smooth Polynomial Additional Thickness Distributions which Emphasize Leading Edge Profile and which Vary Linearly at the Trailing Edge. Aerophysics Research Corporation TN-197. March 1975.

9. Merz, A.W. and Hague, D.S. Theoretical Effect of Modifications to the Upper Surface of Two NACA Airfoils using Smooth Polynomial Additional Thickness Distributions which Emphasize Leading Edge Profile and which Vary Quadratically at the Trailing Edge. Aerophysics Research Corporation TN-199. March 1975.

10. Jameson, A. "Transonic Flow Calculations for Airfoils and Bodies of Revolution." Grumman Aerodynamics Report 390-71. December 1971.

11. Hague, D.S., Rozendaal, H.L., and Woodward, F.A. Application of Multivariable Search Techniques to Optimal Aerodynamic Shaping Problems. The Journal of the Astronautical Sciences, Vol. XV, No. 6, pp. 283-296, November-December 1968.